

Testing unit for compliance testing of frequency regulating performance of power-generating modules

Master's thesis in Electric Power Engineering

Johan Olson
Nils Åkesson

MASTER'S THESIS 2021:EENX30

**Testing unit for compliance testing of
frequency regulating performance of
power-generating modules**

JOHAN OLSON
NILS ÅKESSON



CHALMERS
UNIVERSITY OF TECHNOLOGY

Department of Electrical Engineering
Division of Electric Power Engineering
CHALMERS UNIVERSITY OF TECHNOLOGY
Gothenburg, Sweden 2021

Testing unit for compliance testing of frequency
regulating performance of power-generating modules

© JOHAN OLSON, NILS ÅKESSON, 2021.

Supervisor: Andreas Petersson, Protrol Engineering AB
Examiner: Massimo Bongiorno, Department of Electrical Engineering, Chalmers

Master's Thesis 2021:EENX30
Department of Electrical Engineering
Division of Electric Power Engineering
Chalmers University of Technology
SE-412 96 Gothenburg
Telephone +46 31 772 1000

Cover: Test principle of a power-generating module and the testing unit for compliance testing of frequency regulating performance.

Typeset in L^AT_EX
Printed by Teknologtryck
Gothenburg, Sweden 2021

Testing unit for compliance testing of frequency
regulating performance of power-generating modules

JOHAN OLSON

NILS ÅKESSON

Department of Electrical Engineering
Chalmers University of Technology

Abstract

With more renewable energy sources and a decreasing amount of inertia in the power system the frequency deviations increase in amount and magnitude. New and updated regulations regarding frequency regulation increases the requirements of the performance of a power-generating module's frequency regulation. The requirements also increase the demand of testing the power-generating module's compliance with the new regulations.

The project has developed a testing unit with the purpose of testing a power generation module's performance due to frequency deviations in the power system. The testing unit's functions is to measure active power output of a power generation module as well as providing a simulated frequency signal, representing the grid frequency.

The software of the testing unit has been simulated in an ideal case together with a simple power-generating module model consisting of a hydro turbine governor, an exciter and a generator. The simulated voltages and currents from the generator have later been realised using variable voltage sources, used to test the hardware performance of the testing unit.

The results shows a testing unit that fulfills it's purposes but also the importance of using the correct parameters in the governor depending on the purpose of the power-generating unit. The method of the project differs from the real application method but shows how to, in a safe manner, control a simulated model of a power-generating module with external equipment.

Keywords: Frequency, RfG, FCR, PLL, Governor, Power-generating module, Speed droop, Simulink, Matlab.

Testing unit for compliance testing of frequency
regulating performance of power-generating modules
JOHAN OLSON
NILS ÅKESSON
Department of Electrical Engineering
Chalmers University of Technology

Sammanfattning

Med mer förnyelsebara energikällor och en minskande tröghetsmassa i kraftsystemet ökar frekvensavvikelsena både i antal och i amplitud. Nya och uppdaterade föreskrifter och regulationer avseende frekvensreglering ökar kraven som ställs på en kraftproduktionsmoduls prestanda av frekvensreglering. De ökar också efterfrågan på att testa hur väl kraftproduktionsmodulen följer de nya kraven.

Projektet har utvecklats en testutrustning med syftet att testa en kraftmoduls prestanda att reglera aktiv uteffekt givet en frekvensavvikelse i kraftsystemet. Testutrustningens funktioner är att mäta aktiv effekt av en kraftproduktionsmodul samt försöka den med en simulerad frekvenssignal som representerar nätfrekvensen. Testutrustningens mjukvara har simulerats under ideella förhållanden med en enkel kraftproduktionsmodul bestående av en vattenkraftregulator, spänningsregulator och en generator. De simulerade spänningarna och strömmarna från generatoren har därefter realiserats med kontrollerbara spänningskällor för att testa testenhets hårdvaruprestanda.

Resultaten visar att enhetens syften är uppfyllda samt vikten av att använda rätt parametrar i turbinregulatorn beroende på kraftproduktionsmodulens syfte. Metoden i projektet skiljer sig från tillämpningen vid ett riktigt test men visar på hur, på ett säkert sätt, en simulerad kraftproduktionsmodul kan kontrolleras med extern utrustning.

Keywords: Frekvens, RfG, FCR, PLL, Turbinregulator, Kraftproduktionsmodul, Speed droop, Simulink, Matlab.

Acknowledgements

We would like to thank Andreas Petersson and Torbjörn Karlsson who have been our guides along the way with implementing code and helping us understand it's purpose. Thank you, Professor Massimo Bongiorno and Associate Professor Peiyuan Chen for your interest and help with equipment used for tests at Chalmers. All employees at Protrol have our shared gratitude for their support and offering us a great work environment.

"Att mäta är att veta" - Evert Agneholm

Johan Olson and Nils Åkesson, Gothenburg, February 2021

Contents

List of Acronyms	xiii
List of Figures	xv
List of Tables	xvii
1 Introduction	1
1.1 Background	2
1.1.1 Requirements for Generators (RfG)	2
1.1.2 Nordic frequency market	3
1.1.3 Electrical preparedness - island operation	5
1.1.4 Testing unit platform	5
1.2 Aim	5
1.3 Problem definition	6
1.4 Limitations	6
1.5 Sustainability aspects	7
1.5.1 Social aspects	7
1.5.2 Ecological aspects	8
1.5.3 Economic aspects	8
2 Frequency control	9
2.1 Inertial response of synchronous machines at frequency deviations	10
2.2 RfG limitations	11
2.3 Frequency Containment Reserve	12
2.4 Technical requirements for testing of FCR provision in the Nordic synchronous area	12
2.5 Governor and speed droop control	13
3 Test principle	15
3.1 Open loop operation	16
3.2 Closed loop operation using hardware-in-the-loop	17
4 Protrol's testing unit	19
4.1 Hardware	19
4.1.1 Sample rate of output file	20
4.2 Web interface	21
4.3 Software development tool	21

4.4	Signal processing and software implementation	21
4.4.1	Synchronous coordinates	21
4.4.2	Phase locked loop	23
4.4.3	Instantaneous active and reactive power	25
4.4.4	Island operation and closed loop simulation	26
4.4.5	Discrete time low pass filter	27
5	Performance testing	29
5.1	Measuring precision	29
5.1.1	ONLY-AT633 and OMICRON CMC 356	30
5.2	Grid testing	31
5.3	Application testing	32
5.3.1	Simulation model in Simulink	33
5.3.2	Simulation environment and software to hardware interface . .	36
5.3.3	Amplifier equipment	36
6	Results	37
6.1	Precision tests	37
6.2	Grid tests	40
6.3	Application tests	41
6.3.1	Open loop operation	42
6.3.2	Closed loop operation	48
7	Discussion	51
7.1	Precision of measurements	51
7.2	Deviation between measured and simulated values in the application testing	52
7.3	Simulated power-generating module or real power-generating module	52
7.4	Importance of parametrisation of the governor	53
7.5	Future studies	53
8	Conclusion	55
	Bibliography	57

List of Acronyms

AC	Alternating current
ADC	Analog-to-digital converter
aFRR	Automatic frequency restoration reserve
CPU	Central processing unit
DAC	Digital-to-analog converter
DC	Direct current
ECU	Electronic control unit
EIFS	Energimarknadsinspektionens författningssamling
FCR	Frequency containment reserve
FCR-D	Frequency containment reserve-disturbance
FCR-N	Frequency containment reserve-normal
FFR	Fast frequency reserve
HVDC	High-voltage direct current
HWIL	Hardware-in-the-loop
IDE	Integrated development environment
MCPU	Master controller processor unit
mFRR	Manual frequency restoration reserve
PCB	Printed circuit board
PLL	Phase locked loop
RfG	Requirements for generators
TSO	Transmission system operator

List of Figures

1.1	Frequency of the Nordic synchronous system sampled at 10 Hz for 24 hours, 2019-03-04. The data was collected by Fingrid at a 400 kV substation in Kangasala with local time (UTC+2) [8].	3
1.2	Frequency of the Nordic synchronous system during 10 minutes from 12:00 in Figure 1.1 [8].	4
1.3	Frequency of the Nordic synchronous system during 4 minutes from 14:04 in Figure 1.1, with frequency drop to 49.591 Hz at 14:05:26 [8].	4
2.1	The frequency reserve activation process [12].	9
2.2	Ideal steady-state characteristics of a governor with speed droop control. . .	14
2.3	Simple governor model with a PI regulator including a speed droop feedback. .	14
3.1	Principle description of test equipment connection.	16
3.2	A step test sequence.	16
3.3	An imposed sinusoidal test sequence.	17
3.4	Schematic for island operation testing with HWIL.	17
3.5	A load step for island operation simulation.	18
4.1	Layout of the testing module.	20
4.2	Transformation from a three-phase system into $\alpha\beta$ and dq-frame.	22
4.3	Block diagram of a phase locked loop [17].	23
4.4	Bode plot of the PLL described in Section 4.4.2.	25
4.5	Measurement and tracking system including a Clarke transformation, a Park transformation and a PLL.	25
5.1	Test setup with relay tester ONLLY-M783 and OMICRON CMC 356. Dotted lines are operations made in software and full lines are physical cables. . .	29
5.2	Test setup with grid connection. Dotted lines are operations made in software and full lines are physical cables.	31
5.3	Test setup with physical measurements. The simulated strong grid voltage is sent out with the DAC in MicroLabBox and the current comes from a amplified voltage from TC.ACS sent through a known resistor. Dotted lines are operations made in software and full lines are physical cables.	32
5.4	Simulink model of the power-generating module and the testing module. . .	34
6.1	Phase voltage U_b at 50.1 Hz, with 2 kHz sampling frequency.	37
6.2	Active power and frequency sampled at 2 kHz.	38
6.3	Step of active power and frequency with an output sample rate of 2 kHz. .	38
6.4	Step of active power and frequency with an output sample rate of 50 Hz. .	39

6.5	Active power at frequencies of 50.005 Hz and 50.1 Hz consecutively, sampled at 2 kHz and then being down-sampled to 50 Hz.	39
6.6	Active power and frequency of resistive load connected to grid, sampled with 2 kHz.	40
6.7	Steady state active power with offset between simulated and measured values.	41
6.8	Steady state active power with compensated offset.	41
6.9	+0.1 Hz frequency step with open loop operation of the testing unit.	42
6.10	+0.2 Hz frequency step with open loop operation of the testing unit.	43
6.11	+0.5 Hz frequency step with open loop operation of the testing unit.	43
6.12	-0.1 Hz frequency step with open loop operation of the testing unit.	44
6.13	-0.5 Hz frequency step with open loop operation of the testing unit.	44
6.14	-0.5 Hz frequency step with open loop operation of the testing unit after reaching maximum capacity.	45
6.15	+0.1 and -0.2 Hz frequency step sequence with open loop operation of the testing unit.	45
6.16	+0.2 and -0.3 Hz frequency step sequence with open loop operation of the testing unit.	46
6.17	60 sec period time imposed sinusoidal frequency change with amplitude deviation of ± 0.1 Hz, with open loop operation of the testing unit.	46
6.18	30 sec period time imposed sinusoidal frequency change with amplitude deviation of ± 0.1 Hz, with open loop operation of the testing unit.	47
6.19	10 sec period time imposed sinusoidal frequency change with amplitude deviation of ± 0.2 Hz, with open loop operation of the testing unit.	47
6.20	+0.1 Hz frequency step with open loop operation of the testing unit with governor parameter K_i set to 0.07.	48
6.21	-1 MW load step with closed loop operation of the testing unit.	48
6.22	+1 MW load step with closed loop operation of the testing unit.	49
6.23	+1 MW load step with closed loop operation of the testing unit. Simulated and measured active power crossing.	49
6.24	-1 MW load step with closed loop operation of the testing unit with governor parameter K_i set to 0.7.	50
6.25	+1 MW load step with closed loop operation of the testing unit with governor parameter K_i set to 0.7	50
7.1	Active power at frequencies of 50.005 Hz and 50.1 Hz consecutively sampled at 2 kHz, unfiltered and filtered, being down-sampled to 50 Hz.	51

List of Tables

2.1	Proposal of maximum capacity thresholds for power-generating modules in the Nordic synchronous system.	11
2.2	Minimum time period for which a power-generating module in Nordic countries has to be capable of operating at different frequencies, deviating from a nominal value, without disconnecting from the grid [5].	11
2.3	Volume requirements of regulating power for the countries in the Nordic power system.	12
4.1	Processors and clock oscillator of the testing unit.	19
4.2	Ports of the testing unit.	20
4.3	Different values of K for different applications of the Clarke transformation [17].	22
4.4	Parameter selection for the PLL.	24
5.1	ONLY-AT633 technical specification.	30
5.2	OMICRON CMC 356 technical specification.	30
5.3	States triggered from different binary inputs of the testing unit.	33
5.4	Selected parameters in the generator of the Simulink model.	34
5.5	Selected parameters in the governor of the Simulink model.	35
5.6	Testing unit DAC output voltage and corresponding frequency value for simulated governor input.	35
5.7	TC.ACS technical specification.	36

1

Introduction

Today, the climate change forces the society to change to more carbon neutral energy sources even though the production of power will vary more and introduce more instability to the system compared to before. The process of replacing the conventional thermal and nuclear power plants with renewable production units brings challenges to the system. When removing the base production units and replacing them with power electronic controlled power-generating modules, the total system inertia decreases. Less inertia means less energy stored in the system and during power imbalances there will be faster deviations in frequency compared to power systems which has a higher amount of inertia [1].

Renewable energy sources follow a certain long-term pattern such as more wind hours during winter and more sun hours during the summer. The short-term pattern is more random due to rapid weather changes which causes imbalances in the power system and needs to be compensated for with control equipment and production units.

The load characteristic of the power system is seeing a shift as new technology has been established and changes the way the loads act. The introduction of variable speed drives make induction motors act as a constant power sources and disconnects the spinning reserves of kinetic energy from the system [2].

The fluctuating power generation combined with less inertia causes stress on the system when balancing the supply to the demand. Frequency in the power system is a measurement of how well the supply and demand are matched and the system is designed to operate at 50 Hz. The tripping of large production units or high-voltage direct current (HVDC) links are often the reason for large fluctuations and might, in the worst-case scenario, cause the frequency to drop to unacceptable levels. Off-limit frequencies might lead disconnection of power-generating modules and loads, producing a cascade effect and widespread power outages [3].

Frequency stability is the power system's ability to maintain a steady frequency after a severe system disturbance resulting in an imbalance between the generation and the load. To cope with the ongoing transition to a more renewable reliant power production, the control equipment for frequency stability needs to be simulated and validated for different dynamic scenarios. The market for speed droop, ramping, frequency control reserve and disturbance power reserve will continue to grow with more renewables along with validation of the frequency control equipment [4].

1.1 Background

New regulations, made to ensure the quality of power-generating module operation and grid stability, has been established for power producers in Europe. The need to test power-generating modules is more dire now as verifying unit function is mandatory to enforce the regulations.

1.1.1 Requirements for Generators (RfG)

In 2016, the European commission released regulations for establishing a network code on requirements for grid connection of generators (RfG). The requirements are set to bring harmonised standards that generators must respect in order to connect to the grid [5].

RfG should:

- Establish new rules for the interconnection of power generating modules.
- Ensure the power generators ability to contribute to the functionality of the grid.
- Increase the ability to connect renewable power production.
- Harmonise the rules for European power producers.

To reach this goal, all power production units that are rebuilt and/or being newly installed must fulfill certain criterion in order to be connected to the grid. Among these criterion are frequency control, active power output regardless of the change in frequency, droop settings, voltage levels and other boundaries set by the transmission system operator (TSO).

The RfG is developed for the European market, but the regional or domestic markets within Europe may enforce more requirements as long as they are in line with the RfG. In Sweden, these requirements have been further explained in EIFS 2018:2 to be adapted to the Nordic market [6].

1.1.2 Nordic frequency market

The frequency in the Nordic synchronous system fluctuates around the nominal 50 Hz. To cope with these fluctuations, power-generating modules capable of controlling the active power output as a response to system frequency changes are used in the system. The frequency regulating services used in the Nordic market are called frequency containment reserves (FCR) and are divided into FCR-normal (FCR-N) and FCR-disturbance (FCR-D).

- FCR-N is an up- and down-regulating service with low frequency deviation threshold set to be within ± 0.1 Hz from the nominal 50 Hz.
- FCR-D is an up-regulating service that is activated for larger frequency deviations and the threshold is set to be within -0.1 Hz and -0.5 Hz.
- FCR-D down regulation is a product soon to be introduced on the market with the threshold set to be within +0.1 Hz and +0.5 Hz.

Between 2014 and 2019, the daily average numbers of over and under frequency deviations have increased and there have been slightly more FCR-D down threshold crossings (> 50.1 Hz) than under FCR-D up threshold crossings (< 49.9 Hz) for every year during the period [7]. In 2019 the total daily average number of FCR-D threshold crossings were 119. 59 of those were FCR-D up threshold crossings. [7].

Figure 1.1 is showing the frequency of the Nordic synchronous system during 24 hours of the day 2019-03-04. The frequency deviates from the nominal value around ± 0.1 Hz with an exception of a large frequency drop at just after 14:00.

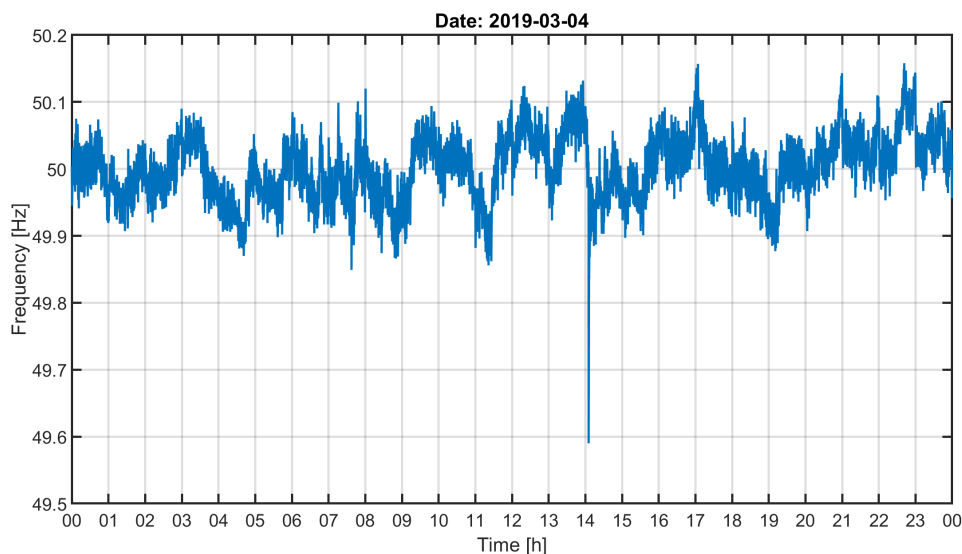


Figure 1.1: Frequency of the Nordic synchronous system sampled at 10 Hz for 24 hours, 2019-03-04. The data was collected by Fingrid at a 400 kV substation in Kangasala with local time (UTC+2) [8].

1. Introduction

The change of load and generation changes constantly, creating a mismatch of active power. Figure 1.2 is a close-up view of Figure 1.1, showing the frequency during 10 minutes.

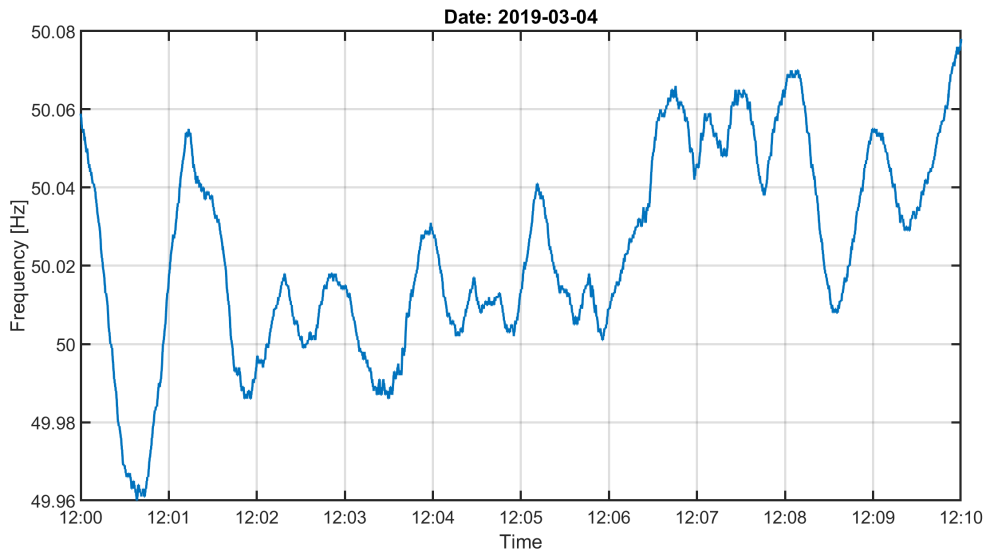


Figure 1.2: Frequency of the Nordic synchronous system during 10 minutes from 12:00 in Figure 1.1 [8].

Figure 1.3 shows the larger frequency drop in Figure 1.1 in a 4 second window where the frequency drops to 49.591 Hz due to a nuclear power plant trip with an active power loss of 1249 MW [7]. The power balance in the system between the load and generation has a direct correlation with the frequency, hence the power deficit in the system from the tripped generating unit causing the large frequency drop.

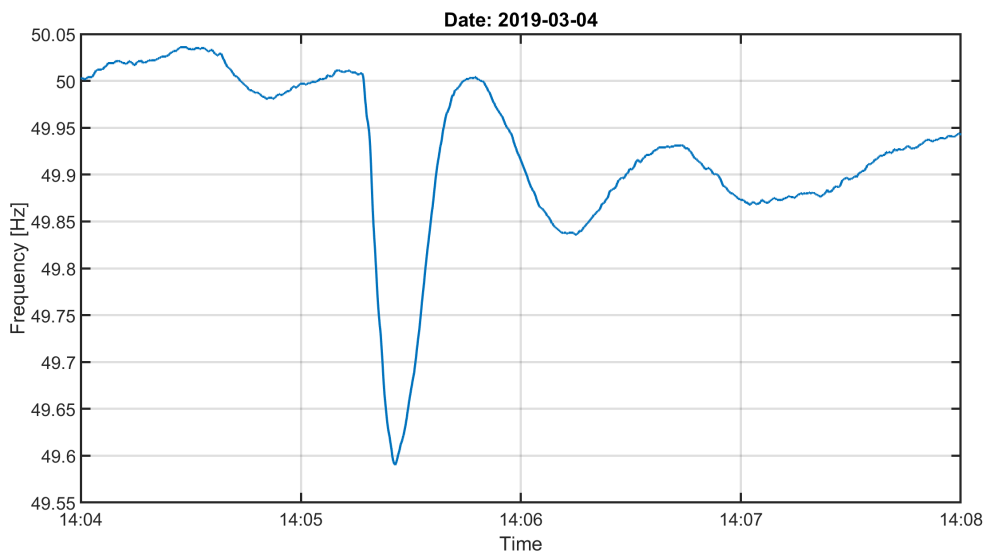


Figure 1.3: Frequency of the Nordic synchronous system during 4 minutes from 14:04 in Figure 1.1, with frequency drop to 49.591 Hz at 14:05:26 [8].

Svenska Kraftnät, the electricity transmission system operator (TSO) of Sweden, had a

net cost of 1302 MSEK for FCR services in 2019 [9]. There is a high need to validate FCR capability of the providers' power-generating modules, as the market involves substantial amount of money while having uncertainties regarding the performance of the reserves.

1.1.3 Electrical preparedness - island operation

The government or the TSO for a regional power system is responsible for the electrical preparedness. This means that they should ensure that the electricity supply is prepared for events such as war, terrorism and natural disasters. One way of ensuring regional electricity supply is to make the power-generating modules in a system able to run in island operation. Island operation is when power-generating modules along with electricity users are operated in a geographical delimited electrical network, disconnected from the surrounding power grid [10].

The requirements and operation plans are often classified and can be different for every power-generating module or regional network of modules. This makes a generic test case difficult to describe, although the island operation capability of the frequency control power-generating modules needs to be tested.

1.1.4 Testing unit platform

Protrol is developing a testing unit for compliance testing of frequency regulating services of power-generating modules.

The testing unit is based upon Protrol's fault detectors used for monitoring, controlling and analysing of the distribution grid. By expanding the platform of the fault detectors with voltage measuring equipment and a digital-to-analog converter (DAC) port, equipment for compliance testing can be achieved.

1.2 Aim

The aim of the project is to develop, construct and implement functions in Protrol's platform to test the frequency controlling capability of a power-generating module. The tests to be performed are to evaluate the performance, such as speed and sensitivity, of a power-generating module under test.

1.3 Problem definition

With the regulations and requirements for testing of a power generating module, the main question becomes:

How is the frequency regulating performance of a power generating module tested to ensure the requirements of its application are met?

The focus is to develop a testing unit for validating the frequency control capabilities of type C and D power-generating modules, with regard to the regulations of RfG, FCR and island operation. The testing unit should be able to measure the active power output and send a simulated frequency signal to a power-generating module. The project is divided into the following parts:

- Implementation of desired test methods in Protrol's platform.
- Testing of measuring performance of the testing unit.
- Development and implementation of a simulation model of the testing unit and a power-generating module in Simulink.
- Real time simulations with a power-generating module model for application testing of the testing unit.

The chosen method of using simulations instead of measuring on a real power-generating module may differ in the way the input signals to the testing unit behaves.

1.4 Limitations

The limitations of the project are:

- The project will not include any designing of the printed circuit boards (PCBs) used within the testing unit nor will it include writing the user interface of the testing module, as this is provided by the Protrol product development team.
- The guidelines and regulations used for the project will be ones made for the European market and if applicable more specifically the Nordic synchronous system.
- The project will focus on implementing functions for FCR services and leave other frequency regulating services outside the scope.
- Power-generating modules of type A and B will not be investigated as these are smaller units not required by RfG to provide frequency controlling services.
- Frequency dependent loads are not taken into account in closed loop operation simulations.

1.5 Sustainability aspects

In order to enforce a certain level of integrity in the report and during the project, the authors are following the IEEE Code of Ethics [11]. Here, ten guidelines are provided to ensure that the work is conducted at the highest professional and ethical cautious manner, where some are more prominent for the project at hand.

"5. to seek, accept, and offer honest criticism of technical work, to acknowledge and correct errors, to be honest and realistic in stating claims or estimates based on available data, and to credit properly the contributions of others;" [11].

Since the work is to be carried out at Protrol and is evolved around the company's products, it is necessary to acknowledge the material and help received from Protrol as well as crediting other sources of information used in the project in order to ensure total transparency.

"3. to avoid real or perceived conflicts of interest whenever possible, and to disclose them to affected parties when they do exist;" [11].

As the master's thesis is conducted at Protrol, the authors have responsibility towards Protrol and Chalmers University of Technology, meaning any flaws or implication found in the project and its end product should be disclosed and discussed between both parties. This both to give Protrol the chance of eliminating and/or avoiding any faults in their products and to give the seat of learning from Chalmers the full insight concerning pitfalls regarding future works in the area.

1.5.1 Social aspects

By ensuring that a power-generating module is up to par with the high standard of operation the network code has set, more renewable sources can be integrated into the grid without compromising the stability. Since most renewable sources fluctuate in production as they are dependent of the environment (sun, wind and waves) they are inherently unstable in output power and or frequency. Assuring the high operating standard is therefore key to foresee and provide the needed generation with given environmental circumstances and power demand from the market.

Introducing a power-generating module testing unit, which can be permanently installed and remotely operated, will pave way for more frequent testing of a module's operating condition. With a grid powered only by highly functioning modules, the stability of the grid will increase and further contribute to less power outages, giving the end users safety and increased quality of life.

1.5.2 Ecological aspects

Regulations such as RfG are meant to ease the integration of renewable power production and enable more efficient use of the existing grid. By enabling the shift from old energy sources to new renewable ones without losing the stability in the grid is key for a smaller carbon footprint in a society run on electricity. By ensuring that modules are functioning in accordance with the specified criterion, the need for buying power from regions with less renewable sources when demand is higher than local production is also reduced.

1.5.3 Economic aspects

The process of testing a power-generating module today is time consuming as the test equipment is ungainly and the process of setting up the equipment, testing and disassemble everything once done may take days in man hours. When utilising a permanently installed module which can take measurements remotely, the total testing time is substantially reduced.

The regulations in the RfG states that all newly installed power-generating modules are to be tested as well as older modules which are being rebuilt or modified. By testing the power-generating modules more frequently, occurring faults or non-optimized control parameters may be found, which in turn can lead to less maintenance/repairation costs.

2

Frequency control

The frequency in the power system is an indicator of how well the active power supply matches the demand. The Nordic synchronous system is designed to run at 50 Hz as long as the system is in balance. Whenever there is a deviation from 50 Hz, different types of reserves are activated to get the frequency back to its nominal value. The reserves differ mainly in response time and maximum duration of delivery. For the market, these reserves are traded hourly with a certain amount of regulating power for the area. Figure 2.1 shows the frequency reserve activation process with the activation time range and level of activation due to a frequency deviation.

The abbreviations stand for:

- FFR - Fast Frequency Reserve.
- FCR - Frequency Containment Reserve.
- aFRR - automatic Frequency Restoration Reserve.
- mFRR - manual Frequency Restoration Reserve.

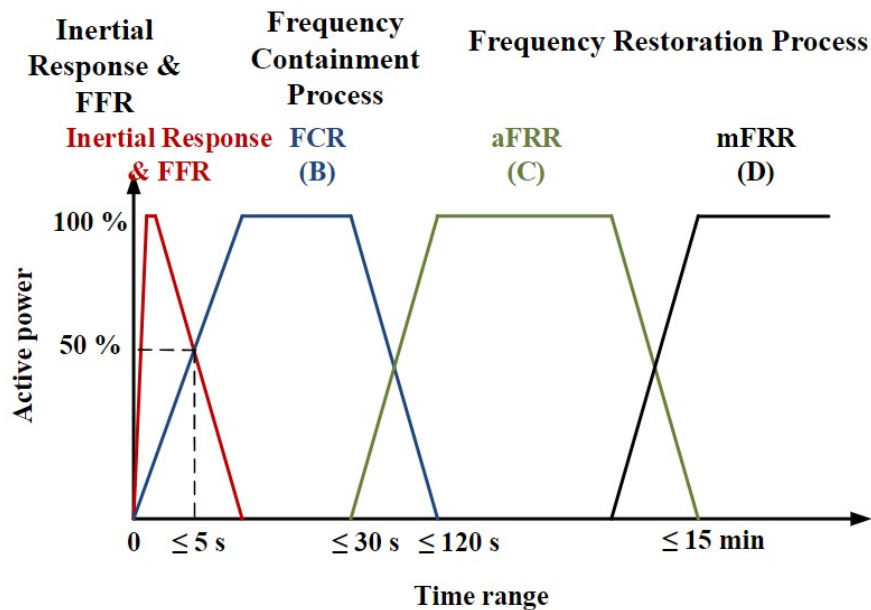


Figure 2.1: The frequency reserve activation process [12].

2.1 Inertial response of synchronous machines at frequency deviations

The inertial response is a physical property of a power-generating module due to a frequency deviation. A kinetic energy, W_k , is stored in the rotating mass of all synchronous modules in the system and is released or obtained at a frequency deviation. The inertial response occurs instantaneous and no control signals are needed. The kinetic energy in the system at a certain point can be described with

$$W_k(t) = \frac{1}{2}J\Omega_r(t)^2, \quad (2.1)$$

$$\Omega_r(t) = \frac{\omega_r(t)}{p}. \quad (2.2)$$

Ω_r is the mechanical speed, ω_r the electrical speed, p the pole pairs and J the inertia of all power-generating modules in the system. In steady state, the mechanical power, P_m , matches the electrical power, P_e , as

$$\Delta P(t) = P_m(t) - P_e(t), \quad (2.3)$$

$$\frac{dW_k(t)}{dt} = \Delta P(t) = 0. \quad (2.4)$$

In non steady state the dynamic behaviour is studied using

$$\frac{dW_k(t)}{dt} = \Delta P(t). \quad (2.5)$$

Combining (2.1) and (2.5) gives

$$J\Omega_r(t)\frac{d\Omega_r(t)}{dt} = \Delta P(t). \quad (2.6)$$

Now J can be rewritten with (2.1) which gives

$$\frac{d\Omega_r(t)}{dt} = \frac{\Delta P(t)}{J\Omega_r(t)} = \frac{\Delta P(t) \cdot \Omega_r(t)}{2W_k(t)}. \quad (2.7)$$

The frequency, f , is proportional to Ω_r and rewriting (2.7) gives

$$\frac{df}{dt} = \frac{d\Delta f(t)}{dt} = \frac{\Delta P(t) \cdot f(t)}{2W_k(t)}. \quad (2.8)$$

To study a single or a small group of units in a system, disconnected from the larger grid, known as island operation an inertia constant, H , is introduced. It is based on the rated power, S_n , and the rated kinetic energy, W_n . H is derived from the rated mechanical angular speed, Ω_n , of the machine(s) included in the island as in

$$H = \frac{W_n}{S_n} = \frac{\frac{1}{2}J\Omega_n^2}{S_n}. \quad (2.9)$$

Combining (2.8) and (2.9) gives the rate of change of frequency,

$$\frac{df(t)}{dt} = \frac{d\Delta f(t)}{dt} = \frac{\Delta P(t) \cdot f(t)}{2 \sum S_n \cdot H_n}. \quad (2.10)$$

2.2 RfG limitations

RfG propose that power-generating modules are to be divided into types based on their maximum capacity threshold, where different geographic regions may have different limits for each type. In the Nordic countries the proposal for the limit is shown in Table 2.1 [5].

Table 2.1: Proposal of maximum capacity thresholds for power-generating modules in the Nordic synchronous system.

Type of module	A	B	C	D
Max capacity threshold	<1.5 MW	1.5 MW - 10 MW	10 MW - 30 MW	>30 MW

Some of the requirements in the RfG are set for all types (including type A which is all power-generating modules below the type B threshold). One requirement is the minimum time period for which a power-generating module must be capable of operating at a certain frequency, as can be seen in Table 2.2.

Table 2.2: Minimum time period for which a power-generating module in Nordic countries has to be capable of operating at different frequencies, deviating from a nominal value, without disconnecting from the grid [5].

Synchronous area	Frequency range	Time period for operation
Nordic	47.5 Hz - 48.5 Hz	30 minutes
	48.5 Hz - 49.0 Hz	To be specified by each TSO, but not less than 30 minutes.
	49.0 Hz - 51.0 Hz	Unlimited
	51.0 Hz - 51.5 Hz	30 minutes

In the case of over frequency the active power response is limited by the minimum regulating level of active power. For under frequency the limit is set by maximum capacity of the power-generating module [5].

2.3 Frequency Containment Reserve

The inertia of the system slows down frequency changes but does not bring the frequency back to its nominal value.

The FCR services are mainly consisting of hydro and non-nuclear thermal units. They are activated as soon as the frequency deviations exceeds the threshold for the different services and have different requirements for activation.

Technical requirements regarding FCR-N:

- Frequency deviation for full activation of FCR-N is ± 100 mHz.
- FCR-N shall for a frequency step change be activated up to 63% within 60 seconds and 100 % within 180 seconds [13].

Technical requirements regarding FCR-D:

- Frequency deviation for full activation of FCR-D is -500 mHz.
- FCR-D shall for a frequency step change from 49.9 Hz to 49.5 Hz be activated up to 50% within 5 seconds and 100 % within 30 seconds [13].

A certain amount of regulating power has to be in the Nordic synchronous system for the two services presented in Table 2.3. The volume of FCR-D is based on a potential trip of the largest power-generating module in the system being Oskarshamn 3 with 1450 MW.

Table 2.3: Volume requirements of regulating power for the countries in the Nordic power system.

	FCR-N [MW]	FCR-D [MW]
Energinet (DK2)	17	41
Fingrid	122	294
Statnett	224	542
Svenska kraftnät	237	573
Sum	600	1450

2.4 Technical requirements for testing of FCR provision in the Nordic synchronous area

The qualification of the power generating modules providing FCR regulation shall be renewed:

- At least every five years.
- If the technical requirements or equipment have been changed.

- If the equipment regarding activation of FCR has been modernised [13].

The technical requirements for the testing unit are described in [14] and the logged data file should as a minimum include the following list.

- Instantaneous active power in MW with a resolution of 0.01 MW and an accuracy of 0.5 % of the rated power of the providing entity, or better. The value shall be such, that it covers all active power changes as a result of the FCR activation.
- Measured grid frequency in Hz, with a resolution of 1 mHz and an accuracy of 10 mHz or better.
- Applied frequency signal, with a resolution of 1 mHz and an accuracy of 10 mHz or better.
- Status id indicating which controller parameter set is active, if it can be automatically changed during the test.

2.5 Governor and speed droop control

The testing unit is to be used for FCR compliance testing of power-generating modules, with regulations applied for the Nordic synchronous system. A predominantly part of FCR services in the Nordic system is hydro power, making a hydro power module the suitable simulation model and reference for parameter values.

To provide FCR services with a power generating module connected to the regional synchronous system or running in different operational mode such as island operation requires different parameters for the controlling governor. There are different kind of regulators with different feedback signals and for a hydro power-generating module it can be either the gate position or the active power output. By including a second feedback loop around the regulator itself a speed droop is obtained, the linear behaviour of a speed droop is shown in Figure 2.2.

The speed droop setting, R_G , is calculated with the no-load frequency, f_{NL} , the full load frequency, f_{FL} , and the nominal frequency, f_0 of a power generating module.

$$R_G = \frac{f_{NL} - f_{FL}}{f_0} \quad (2.11)$$

The speed droop links the steady state frequency of the grid with the active power.

$$\Delta P = \frac{\Delta f}{R_G} \quad (2.12)$$

A speed droop setting of 4 % in a 50 Hz system meaning a frequency deviation of 2 Hz needed to change the active power of the generating unit by 100 %. The speed reference would for this case be 104 % and the actual speed 100 %, meaning every 0.04 % change of the speed reference resulting in a 1 % change in active power.

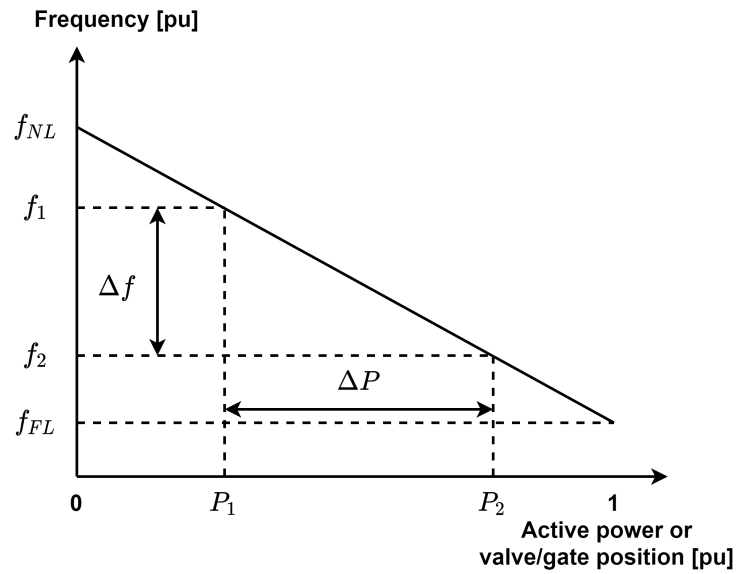


Figure 2.2: Ideal steady-state characteristics of a governor with speed droop control.

It is common to use a PI-regulator to reach the steady state active power output due to a frequency deviation. The governor model shown in Figure 2.3 shows the implementation of a PI-regulator together with a speed droop.

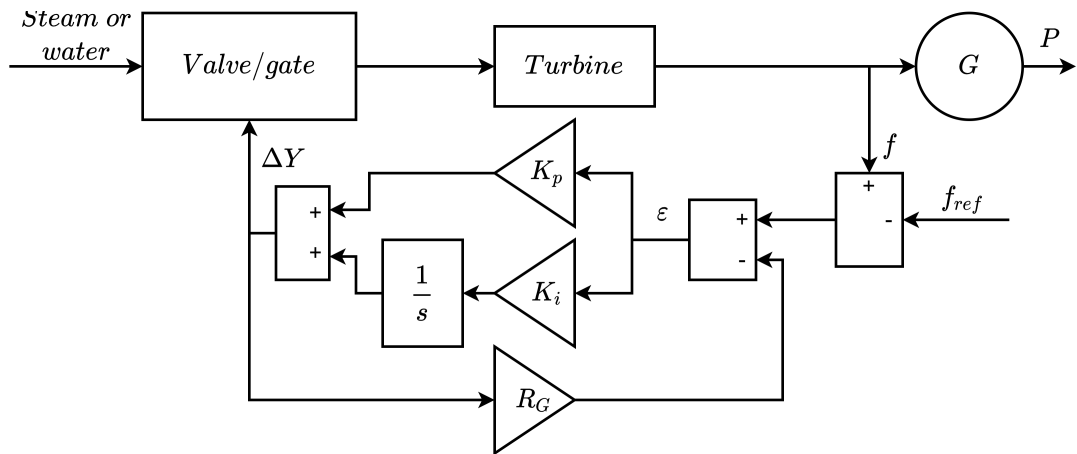


Figure 2.3: Simple governor model with a PI regulator including a speed droop feedback.

Changing values of the regulator parameters K_p and K_i will change how fast the steady state value is reached and how accurate the power generating module is to its reference value.

3

Test principle

The principle of the testing procedure is to study the response of active power output of power-generating module due to a step of the frequency. This is done by replacing the normal grid frequency feedback to the governor with a simulated frequency signal. In order to acquire the entire system response including the governor, the simulated signal is placed outside the governor shown in Figure 3.1 [15]. To obtain the active and reactive power, the voltage and current are measured at the power-generating module's terminal. The operational modes to be tested are a power-generating module in open loop and one in closed loop described in Section 3.1 and 3.2. The difference is that the frequency signal for the open loop operation is based on a set value, while for the closed loop operation it is calculated from the measured active power of the power-generating module and a set value for the load in the system. The power-generating module will always be connected to a strong grid and the response of a changing active power will be due to a changing current.

Using the testing unit to control a real power-generating module without verifying proper functioning and performance of it would be unsafe, as the machine could reach critical operating limits. Therefore the development is first done in software and later realized using DACs, utilising the same principle described in Section 5.3. This method allows function testing of the testing unit in close to ideal conditions while proceeding to add delays and uncertainties in a safe manner.

3.1 Open loop operation

The open loop operation consists of two separate functions for the testing unit, measure power and providing a simulated frequency signal. The frequency signal is set by the user. Figure 3.1 shows the principal setup for this operation mode.

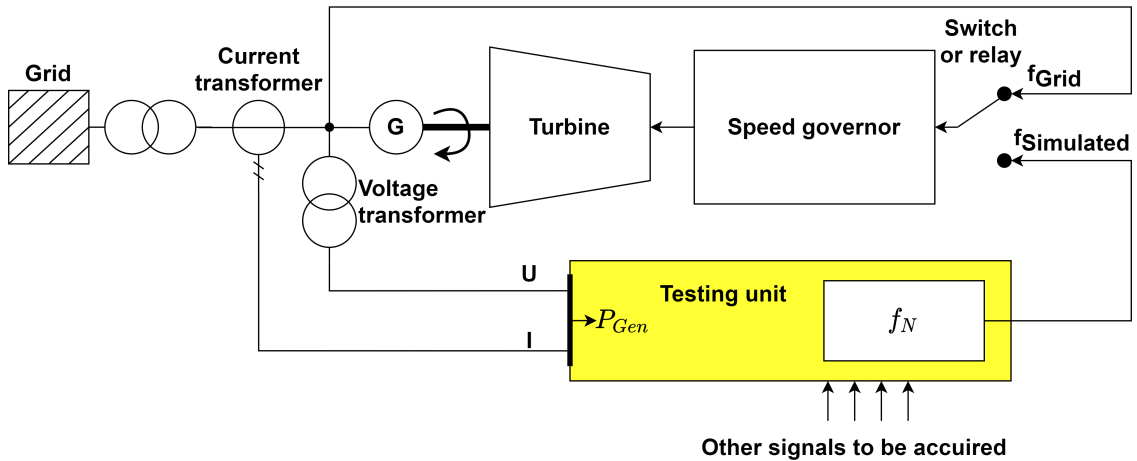


Figure 3.1: Principle description of test equipment connection.

The simulated frequency input to the governor consists of test procedures for control systems:

- Frequency step.
- Imposed sinusoidal frequency variation.
- Frequency variation according to table (t, f) , or a text file.

Figure 3.2 shows a step of the frequency signal that is the input to the governor while Figure 3.3 shows an imposed sinusoidal signal. The response of the power module is mainly analysed from the active power output.

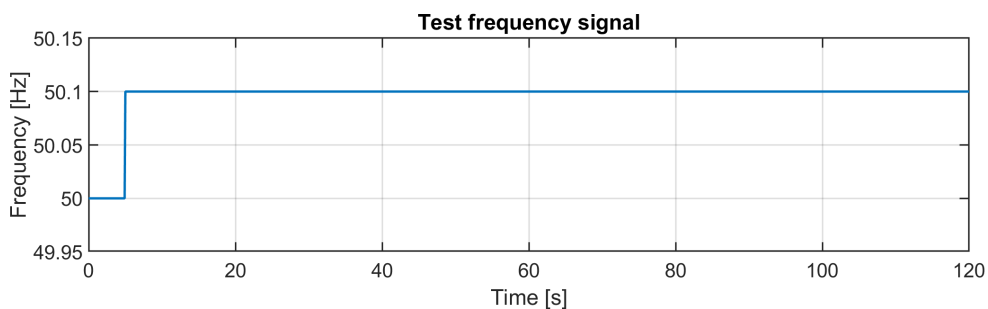


Figure 3.2: A step test sequence.

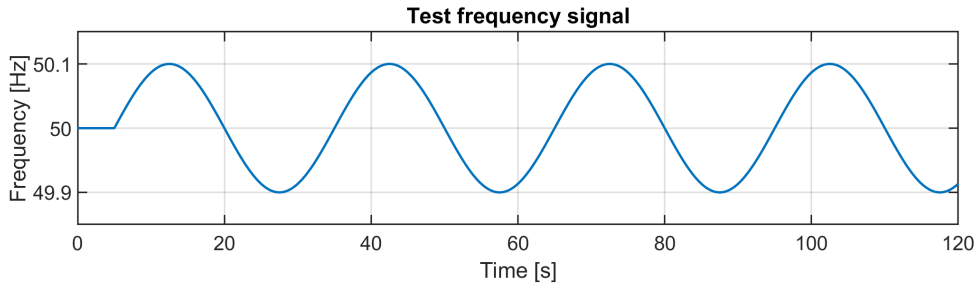


Figure 3.3: An imposed sinusoidal test sequence.

3.2 Closed loop operation using hardware-in-the-loop

Testing with a closed loop operation provides a procedure to test a power-generating module's of island operation performance even though it's still connected to a strong grid. The frequency signal is based on a calculation made from the power imbalance in the simulated island system described in Section 4.4.4. The power imbalance originates from the measured value of the power-generating module and a value of a load set by the user. The method is also denoted hardware-in-the-loop (HWIL) and is shown in Figure 3.4.

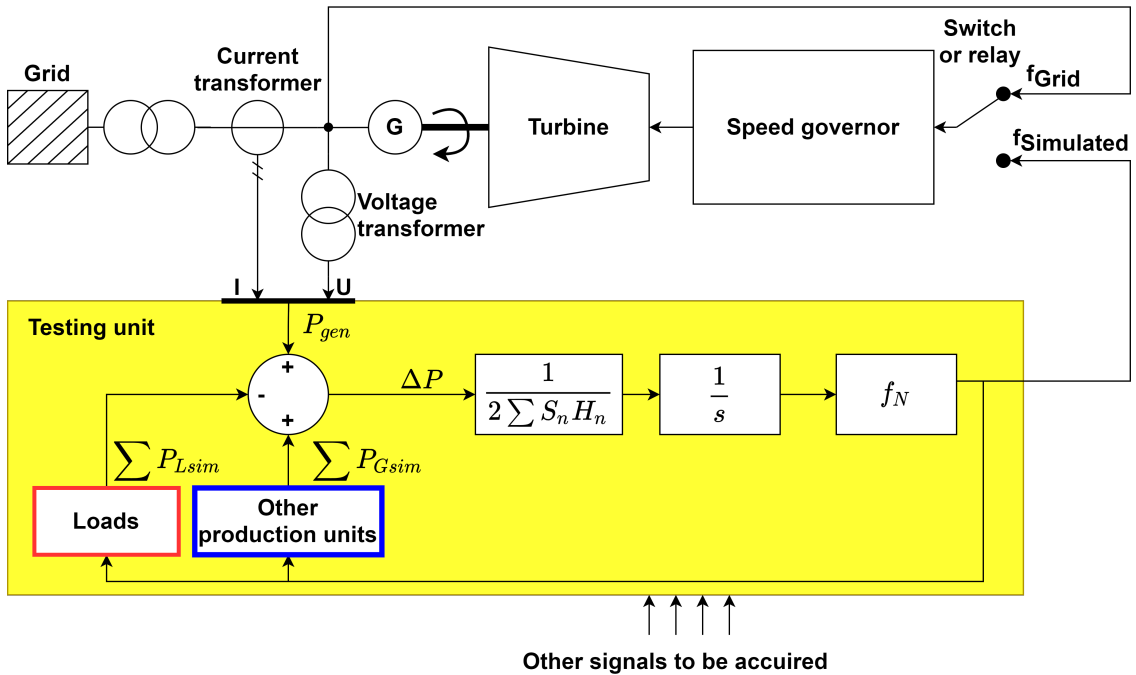


Figure 3.4: Schematic for island operation testing with HWIL.

3. Test principle

The simulated load input to the testing unit consists of test procedures for control systems:

- Load step.
- Load variation according to table (t, f), or a text file.

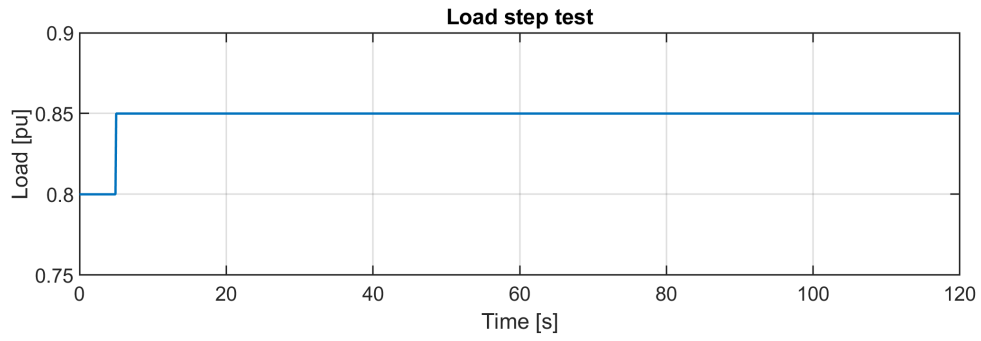


Figure 3.5: A load step for island operation simulation.

4

Protrol's testing unit

The hardware of the testing unit is Protrol's already existing hardware for the product IPC4020 together with the expansion of a new PCB for the application.

4.1 Hardware

The testing unit holds two PCBs, one for current measurements, binary inputs, power supply and auxiliary ports and the other with voltage measurements, analog inputs, binary inputs and the DAC port. The two PCB:s are being run with two central processing units (CPUs) and a clock oscillator.

Table 4.1: Processors and clock oscillator of the testing unit.

Component	Denotion
MCPU	STM32F765VIT6
CPU	STM32F413RGT6
Clock oscillator	HXO-36A

The SRAM memory size of the MCU is 512 Kbytes and the frequency stability of the clock oscillator is 3 ppm.

4. Protrol's testing unit

The ports of the module are of a plug in type and described in Table 4.2 below.

Table 4.2: Ports of the testing unit.

Type of port	Amount of ports	Rating of port(s)
Power supply	1	24-48 VDC
Current measurement	3	5 A
Voltage measurement	4	110 VAC _{L-N}
Voltage measurement	8	10 VAC _{L-N}
Binary inputs	20	24-110 VDC
Binary outputs	4	Breaking capacity 8 A at 250 VAC/30 VDC
Binary outputs	4	Breaking capacity 5 A at 250 VAC/30 VDC
Analog voltage output	1	±10 V
Analog current output	1	± 20 mA
RJ45 communication	1	10/100 Base
USB type B	1	-

The layout of the testing unit is shown in Figure 4.1. The green parts are the different signal ports and the grey parts are the RJ45 and USB type B communication ports. The figure also shows the LEDs of the unit indicating different states [16].

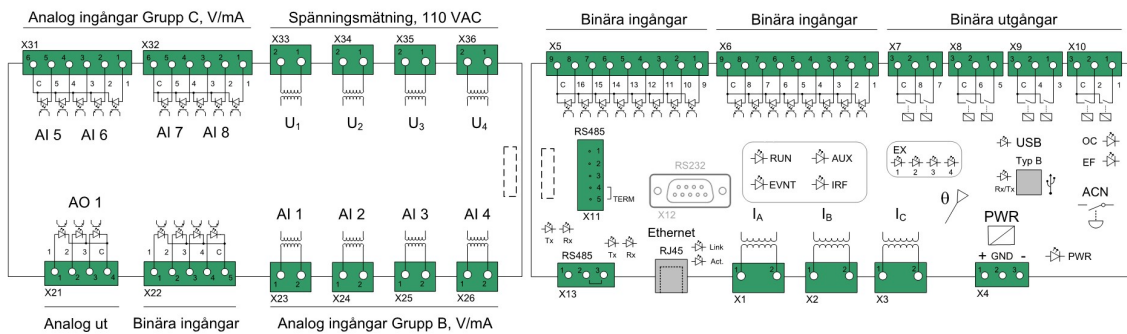


Figure 4.1: Layout of the testing module.

4.1.1 Sample rate of output file

Due to the limitation of storage capacity in the MCU the files with logged data are limited in size. Two lengths of the test are therefore chosen. The short tests log the raw data of 2 kHz and have a total length of 3.05 seconds. The longer tests down samples the output value to every 40:th value giving an output sample rate of 50 Hz and a total length of 122 seconds.

4.2 Web interface

The web interface is reached through the RJ45 or USB connector and is used for monitoring the unit real time or setting settings. The status of binary inputs and outputs, values of measurements and the file with the logged data is reached through the web interface.

4.3 Software development tool

The drivers and implementation of the new hardware are already done and the implementation of new code concerns handling of variables and signals. Atollic TrueSTUDIO is used as the C integrated development environment (IDE). It is an Eclipse based IDE made for development with STM32 processors.

4.4 Signal processing and software implementation

The testing unit's main functionalities are:

- Measure active and reactive power in a circuit.
- Track the grid frequency.
- Provide a simulated frequency signal.

To do so a combination of a phase locked loop (PLL) and synchronous coordinates are used together described in Section 4.4.3. The theory of them individually are first described in Section 4.4.1 and 4.4.2. They are based on the measurement of three phase voltages and currents.

4.4.1 Synchronous coordinates

To simplify analysis of three phase circuits, values are often transformed into the dq-frame. The benefit of having the vectors in this coordinate system is that they will appear as DC quantities in the corresponding reference frames and hence simplify calculations.

First the three phase values are transformed with a Clarke transformation into an equivalent two-phase system with two perpendicular axes, denoted α and β , shown in Figure 4.2.

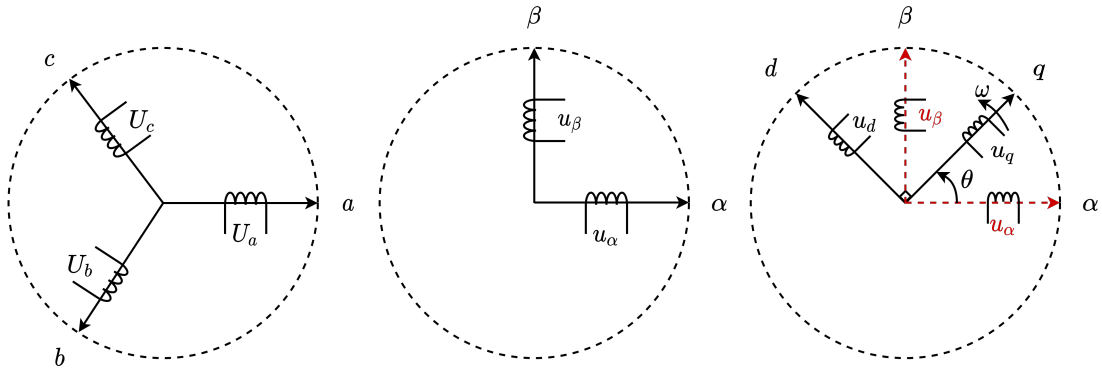


Figure 4.2: Transformation from a three-phase system into $\alpha\beta$ and dq -frame.

The α -axis is considered the real part and the β -axis is the imaginary part in a fixed complex plane. The three-phase/two-phase transformation is expressed as

$$\begin{bmatrix} u_\alpha \\ u_\beta \end{bmatrix} = K \begin{bmatrix} \frac{2}{3} & -\frac{1}{3} & -\frac{1}{3} \\ 0 & \frac{1}{\sqrt{3}} & -\frac{1}{\sqrt{3}} \end{bmatrix} \begin{bmatrix} U_a \\ U_b \\ U_c \end{bmatrix} \quad (4.1)$$

where U_a , U_b and U_c are three-phase voltages, u_α and u_β are the transformed voltages [17]. K is a scaling factor chosen according to the application for the transformation.

Table 4.3: Different values of K for different applications of the Clarke transformation [17].

Application	Peak-value invariant scaling	RMS-value invariant scaling	Power invariant scaling
Value of K	1	$\frac{1}{\sqrt{2}}$	$\sqrt{\frac{3}{2}}$

In the $\alpha\beta$ -frame, the coordinate system is at standstill. Rotating the coordinate system and thus removing the rotation of the vectors in regard to the axes is making the vectors considered fixed phasors. This is called a dq -transformation or Park transformation also seen in Figure 4.2.

From the $\alpha\beta$ -frame, the transformation to the dq -frame is expressed as

$$\begin{bmatrix} u_d \\ u_q \end{bmatrix} = \begin{bmatrix} \cos(\theta) & \sin(\theta) \\ -\sin(\theta) & \cos(\theta) \end{bmatrix} \begin{bmatrix} u_\alpha \\ u_\beta \end{bmatrix}, \quad (4.2)$$

where θ is the angle between the α -axis and the phasor chosen as reference.

The value of K is chosen to be in RMS-value scaling and the θ is provided in equation 4.7 by the Phase Locked Loop described in Section 4.4.2.

4.4.2 Phase locked loop

There are several ways to measure frequency of the grid, here a phase locked loop is used. Figure 4.3 shows a block diagram of a PLL.

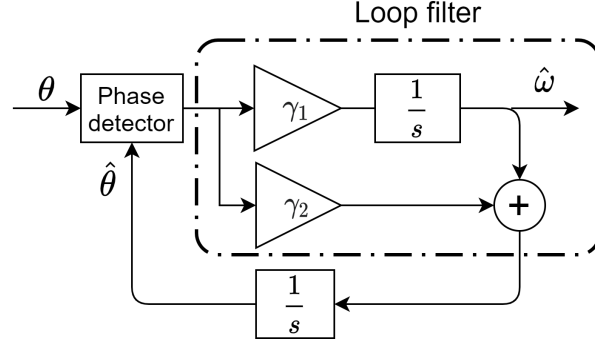


Figure 4.3: Block diagram of a phase locked loop [17].

A PLL is a closed loop estimator to track the speed and position of a vector. The error signal ε from the phase detector can be written as:

$$\varepsilon = \sin(\theta - \hat{\theta}) \quad (4.3)$$

where θ is the rotor position of a synchronous machine and $\hat{\theta}$ is the estimation of the rotor position. The aim of the PLL is to drive the estimate, $\hat{\theta}$, to the same value as θ .

Let us assume that the derivative of the rotor position is the angular velocity, $\dot{\theta} = \omega_r$, in the closed loop system seen in Figure 4.3. With the error signal, ε , fed through the loop filter with gain parameters γ_1 and γ_2 , the estimator equations are introduced, as equation 4.4 and 4.5.

$$\dot{\omega}_r = \gamma_1 \varepsilon \quad (4.4)$$

$$\dot{\hat{\theta}} = \hat{\omega}_r + \gamma_2 \varepsilon \quad (4.5)$$

To get the estimator in discrete form the forward difference approximation is used.

$$\hat{\omega}_{r,k+1} = \hat{\omega}_{r,k} + T_s \gamma_1 \varepsilon_k \quad (4.6)$$

$$\hat{\theta}_{k+1} = [\hat{\theta}_k + T_s (\hat{\omega}_{r,k} + \gamma_2 \varepsilon_k)]_{-\pi}^{\pi} \quad (4.7)$$

For the assumption that $\hat{\theta} \approx \theta$, the PLL is said to be phase locked and thus $\sin(\theta - \hat{\theta}) \approx \theta - \hat{\theta}$ and the estimator equations can be linearized.

$$\dot{\omega}_r = \gamma_1 (\theta - \hat{\theta}) \quad (4.8)$$

$$\dot{\hat{\theta}} = \hat{\omega}_r + \gamma_2 (\theta - \hat{\theta}) \quad (4.9)$$

Expressing the estimator in state space form with $\hat{x} = [\hat{\omega}_r, \hat{\theta}]^T$

$$\dot{\hat{x}} = A \hat{x} + B \theta, \quad (4.10)$$

$$A = \begin{bmatrix} 0 & -\gamma_1 \\ 1 & -\gamma_2 \end{bmatrix}, \quad B = \begin{bmatrix} \gamma_1 \\ \gamma_2 \end{bmatrix}, \quad (4.11)$$

gives the poles by the characteristic polynomial

$$\det(sI - A) = s^2 + \gamma_2 s + \gamma_1. \quad (4.12)$$

The poles can be chosen from the characteristic polynomial

$$(s + \rho)^2 = s^2 + 2\rho s + \rho^2 \rightarrow \gamma_1 = \rho^2, \quad \gamma_2 = 2\rho \quad (4.13)$$

where ρ is considered the bandwidth of the estimator.

To keep a stable system performance of a closed loop system and have a precise forward difference approximation, the recommendation is to select the angular sampling frequency, ω_s , at least 10 times higher than the closed loop bandwidth, ρ .

$$\omega_s \geq 10 \cdot \rho \quad (4.14)$$

Where ω_s comes from the sampling frequency f_s .

$$\omega_s = 2\pi f_s \quad (4.15)$$

According to [18] the transfer function from ε to $\hat{\theta}$ can be described as below, if the system is considered linear and time-invariant.

$$G_{PLL}(z) = \frac{z2\rho T_s + \rho T_s(\rho T_s - 2)}{z^2 + z2(\rho T_s - 1) + \rho T_s(\rho T_s - 2) + 1} \quad (4.16)$$

Where T_s is the sampling time.

$$T_s = \frac{1}{f_s} \quad (4.17)$$

In case of an unsymmetrical grid, the dq-transformed signals described in Section 4.4.1, will contain a negative sequence voltage. The negative sequence component will occur as an oscillation of twice the grid frequency in the dq-frame. For the procedure described in Section 4.4.3 where the u_q phasor is the input signal to the PLL, the choice of a low bandwidth can filter this oscillation out [18].

The parameters chosen in the PLL are:

Table 4.4: Parameter selection for the PLL.

Parameter	f_s	ρ
Value	2000	31.4

This selection of parameters in equation 4.16 will result in a Bode plot shown in Figure 4.4.

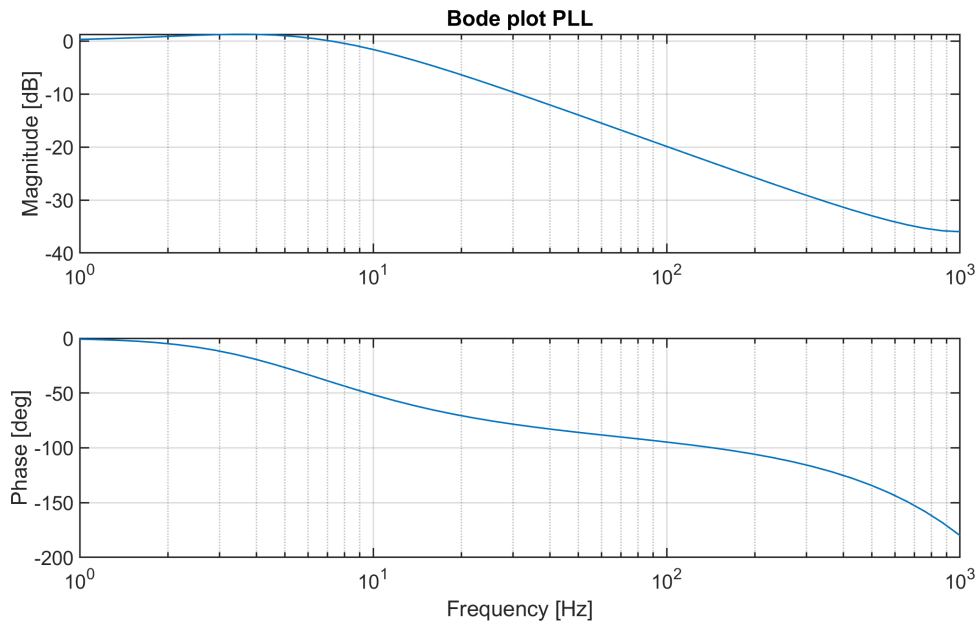


Figure 4.4: Bode plot of the PLL described in Section 4.4.2.

A 100 Hz oscillation in the u_q phasor coming from a negative sequence voltage will then be filtered out -20 dB or 90%.

4.4.3 Instantaneous active and reactive power

Combining the PLL described in Section 4.4.2 with three phase voltage and current measurements transformed into dq-frame a PLL designed for the power system is obtained. Replacing θ in equation (4.2) with the estimated $\hat{\theta}_{k+1}$ in equation (4.7) and using u_q as the input phasor to the PLL will drive u_q to be aligned with the q-axis. Figure 4.5 shows the combination of the techniques.

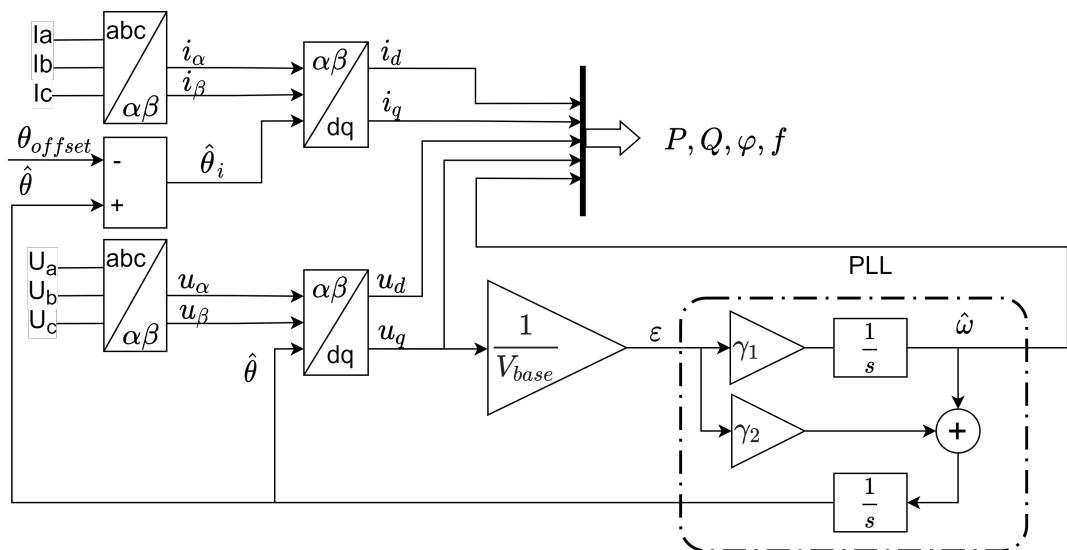


Figure 4.5: Measurement and tracking system including a Clarke transformation, a Park transformation and a PLL.

To calculate the active power, P , reactive power, Q , and the phase difference between voltage and current, φ , measured currents also needs to be in the dq-frame as i_d and i_q [17]. P , Q and φ is then calculated with

$$P = \frac{3}{2K^2}(u_d \cdot i_d + u_q \cdot i_q), \quad (4.18)$$

$$Q = \frac{3}{2K^2}(u_q \cdot i_d - u_d \cdot i_q), \quad (4.19)$$

$$\varphi = \arctan\left(\frac{Q}{P}\right). \quad (4.20)$$

For calibration purposes $\hat{\theta}_{k+1,i}$ in the Park transformation can be adjusted from $\hat{\theta}_{k+1}$ with θ_{offset} .

$$\hat{\theta}_{k+1,i} = \hat{\theta}_{k+1} - \theta_{offset} \quad (4.21)$$

This offset is due to phase shift properties in transformers and hardware filters in the measuring equipment creating a phase shift between the voltage and the current. The ability to calibrate the system is then possible with measuring voltage and current in a fully resistive circuit having θ_{offset} set to zero and calculating φ . The value of φ is then set to θ_{offset} .

The frequency in the circuit is calculated from the estimated speed $\hat{\omega}_{r,k+1}$ in the PLL.

$$f = \frac{\hat{\omega}_{r,k+1}}{2\pi} \quad (4.22)$$

4.4.4 Island operation and closed loop simulation

Island operation refers to a power network running in isolation from the national grid. It consists of at least one power module or HVDC link supplying power to this network, controlling the frequency and voltage.

To test a power-generating module's performance of island operation frequency control the methodology in Section 3.2 is used. The frequency in the system is calculated based on the knowledge of the kinetic energy, W_k , the active power input, $\sum P_{Gsim}$ of other power-generating module(s) and a simulated load curve $\sum P_{Lsim}$. With the measured active power, P_{Gen} , the power imbalance is calculated.

$$\Delta P = P_{gen} - \sum P_{Lsim} - \sum P_{Gsim} \quad (4.23)$$

To describe the Rate-of-Change-of-Frequency (RoCoF) equation (2.10) is used in discrete form.

$$\frac{df_N}{dt} = \frac{\Delta P \cdot f_N}{2 \cdot \sum_{n=1}^M S_n \cdot H_n} \quad (4.24)$$

where M is the amount of units and S_n and H_n are the rated power and the inertia constant of the unit(s). The difference in frequency is based on the sample time T_s between the two samples N and $N + 1$.

$$\Delta f_{N+1} = \frac{df_N}{dt} \cdot T_s \quad (4.25)$$

And the new frequency f_{N+1} is calculated.

$$f_{N+1} = f_N + \Delta f_{N+1} \quad (4.26)$$

4.4.5 Discrete time low pass filter

To smooth out a high frequent or random noise in a measurement signal it's common to use a first order filter. To derive a filter with the backward differentiation method the Laplace transform transfer function is described as

$$H(s) = \frac{y(s)}{u(s)} = \frac{1}{T_f s + 1}. \quad (4.27)$$

Where T_f is the time-constant, u the filter input and y the filter output. Rewriting (4.27) gives

$$T_f s \cdot y(s) + y(s) = u(s). \quad (4.28)$$

Taking the Laplace transform of both sides of equation (4.28) gives the following differential equation.

$$T_f \dot{y}(t) + y(t) = u(t) \quad (4.29)$$

which in discrete form where t_k is considered a point in time is written as

$$T_f \dot{y}(t_k) + y(t_k) = u(t_k) \quad (4.30)$$

The derivative is approximated with the backward differentiation method seen below

$$\dot{y}(t_k) \approx \frac{y(t_k) - y(t_{k-1})}{h} \quad (4.31)$$

where h is the sample time or step size. Combining equation (4.30) and (4.31) then gives

$$T_f \frac{y(t_k) - y(t_{k-1})}{h} + y(t_k) = u(t_k). \quad (4.32)$$

Solving for $y(t_k)$ gives

$$y(t_k) = \frac{T_f}{T_f + h} y(t_{k-1}) + \frac{h}{T_f + h} u(t_k) \quad (4.33)$$

and can be written as

$$y(t_k) = (1 - a)y(t_{k-1}) + au(t_k), \quad (4.34)$$

where the filter parameter usually is written as

$$a = \frac{h}{T_f + h}. \quad (4.35)$$

4. Protrol's testing unit

5

Performance testing

To validate and get the performance of the testing unit, the implemented code is simulated in ideal conditions and the hardware is tested with voltages and currents with a low harmonic content. The last test is a combination of both, where a simulation of a hydro power-generating module is controlled and measured with the testing unit. The goal is to acquire limitations in the implemented code described but also hardware related issues such as delays and noise in the testing unit.

5.1 Measuring precision

To test the precision in the measurements the relay testers described in Section 5.1.1 are used. A predefined sequence is provided to the testing unit changing the voltage level and frequency. This gives a way of testing the response time and precision of the PLL and instantaneous power described in Section 4.4.3. Figure 5.1 shows the setup of the measurement.

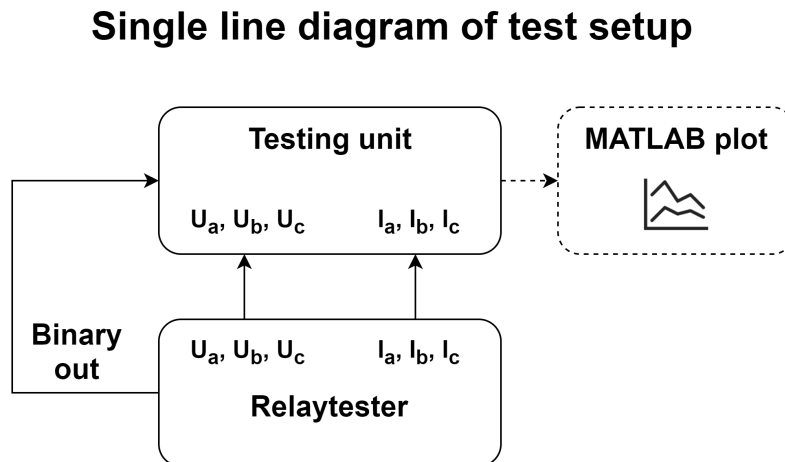


Figure 5.1: Test setup with relay tester ONLLY-M783 and OMICRON CMC 356. Dotted lines are operations made in software and full lines are physical cables.

The logging of the testing unit is activated with a binary input. The sequence of the relay tester is then matched to the length of the output file described in Section 4.1.1.

The calibration of the voltage measurement is done with giving out a direct current (DC) voltage and adjusting the output to the real value.

The voltage is kept at $10 V_{L-N}$, i.e. $V_{Base}=10 V$.

5.1.1 ONLY-AT633 and OMICRON CMC 356

ONLY-AT633 and OMICRON CMC 356 are both relay test units and commissioning tools able to send out both voltages, currents and binary signals on separate channels. They can be programmed to send out predefined sequences where the voltage, current, frequency and binary outputs are controlled over time. Below are the technical specifications.

Table 5.1: ONLY-AT633 technical specification.

Type of port	Nr. of ports	Rating	Accuracy
Current output	3	35 A	<4 mA absolute <0.2 % relative
Voltage output	3	125 V	<4 mV absolute <0.29 % relative
Frequency	-	10-1000 Hz	10 Hz <f <65 Hz not more than +0.001 Hz

Table 5.2: OMICRON CMC 356 technical specification.

Type	Nr. of ports	Rating	Accuracy
Current output	6	32 A	<0.05% reading + 0.02% range
Voltage output	4	400 V	<0.03% reading + 0.01 % range
Binary output	4	6.67 A at 300 V _{AC} 0.17 A at 300 V _{DC}	-
Binary input	10	20-300 V	-
Frequency	-	10-1000 Hz	± 0.5 ppm ± 1 ppm drift

5.2 Grid testing

To test the performance where the frequency and voltage are changing naturally the unit is connected to the grid. To not exceed the rated $115 V_{L-N}$ of the testing unit a measurement transformer rated $400/39 V_{L-L}$ is used. In the current circuit three resistors rated $500 W$ at $240 V$ are used.

Single line diagram of test setup

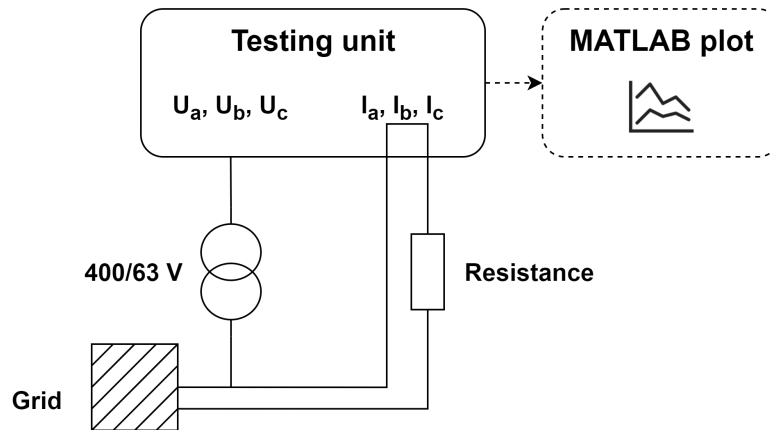


Figure 5.2: Test setup with grid connection. Dotted lines are operations made in software and full lines are physical cables.

Due to a fully resistive circuit the phase shift of the transformer can be compensated following the procedure in Section 4.4.3, along with $V_{Base}=39/\sqrt{3} V$.

5.3 Application testing

To test the testing unit for its application described in Chapter 3 a simulation of a hydro power-generating module is combined with equipment providing voltages and currents. The setup is shown in Figure 5.3 and the individual components are described below.

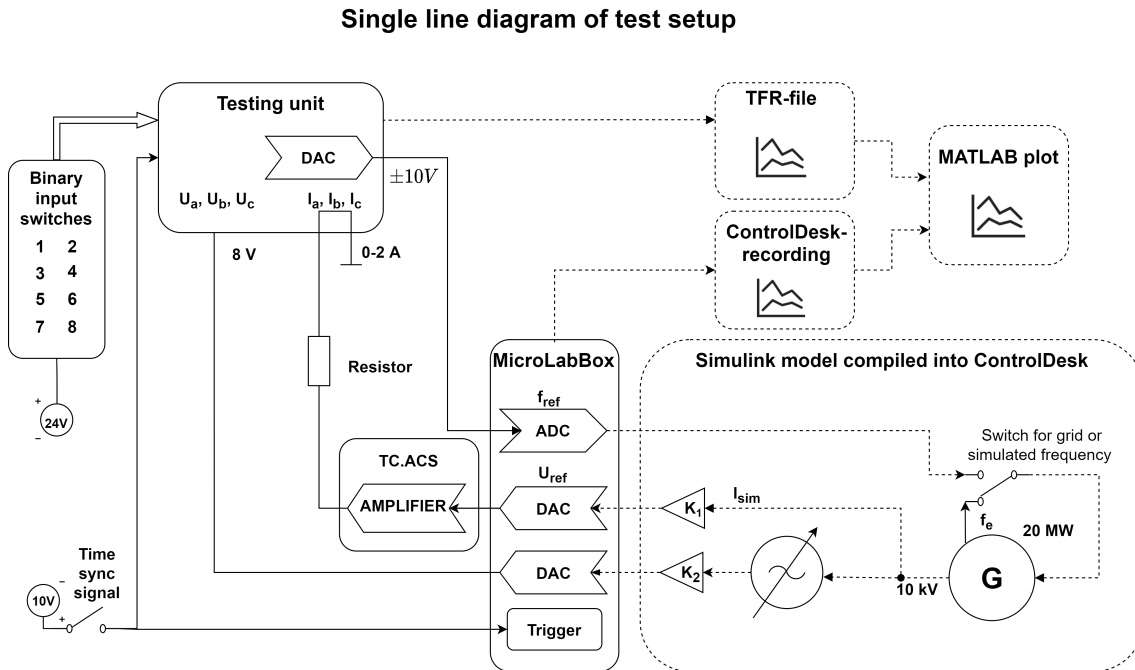


Figure 5.3: Test setup with physical measurements. The simulated strong grid voltage is sent out with the DAC in MicroLabBox and the current comes from a amplified voltage from TC.ACS sent through a known resistor. Dotted lines are operations made in software and full lines are physical cables.

The rated current of the testing unit is 5 A but chosen to be run in a safe region at 0-2 A. For the full setup the voltage output of the TC.ACS will be driving a current through three 50Ω phase resistors. The voltage range of the TC.ACS is then 0-100 V. 100 V represents the rated current of 1154.7 A of the power-generating module in the Simulink model.

To sync the two files extracted from the testing unit and ControlDesk a sync signal is made with a switch. When triggered, a 10 V pulse is sent to both the testing unit and MicroLabBox triggering a recording of a predefined time.

To control the testing unit a physical box with switches triggering binary inputs is also implemented. Depending on which input that is triggered different states are set representing frequency deviations or load steps depending on if the power-generating module is open or closed loop operation.

Table 5.3: States triggered from different binary inputs of the testing unit.

Switch	Deviation from steady state	
	Open loop frequency deviation	Closed loop operation load step
1	+0.2 Hz	+2 MW
2	0 Hz	0 MW
3	+0.1 Hz	+1 MW
4	-0.1 Hz	-1 MW
5	+0.5 Hz	10 MW
6	0.1 Hz set time sinus curve	-0.5 MW
7	Open loop ON	Closed loop OFF
8	Open loop OFF	Closed loop ON

Due to the voltage coming from one source and the current from another the phase difference between them originates in delays and inaccuracies in MicroLabBox and TC.ACS giving out values from the simulation.

5.3.1 Simulation model in Simulink

The simulated results are made in Simulink with a simplified model of a synchronous machine, hydraulic turbine and governor and an exciter in conjunction with an infinite strong grid, all found in the Simscape model library. The reason for having the simulations in Simulink is that it can be compiled into ControlDesk described in section 5.3.2.

The model is developed for two purposes:

- Study the response of a power-generating module in simulation due to a change in frequency.
- Test the code written in the testing unit, to see the performance in ideal conditions.

Figure 5.4 shows a setup of how the model is built.

5. Performance testing

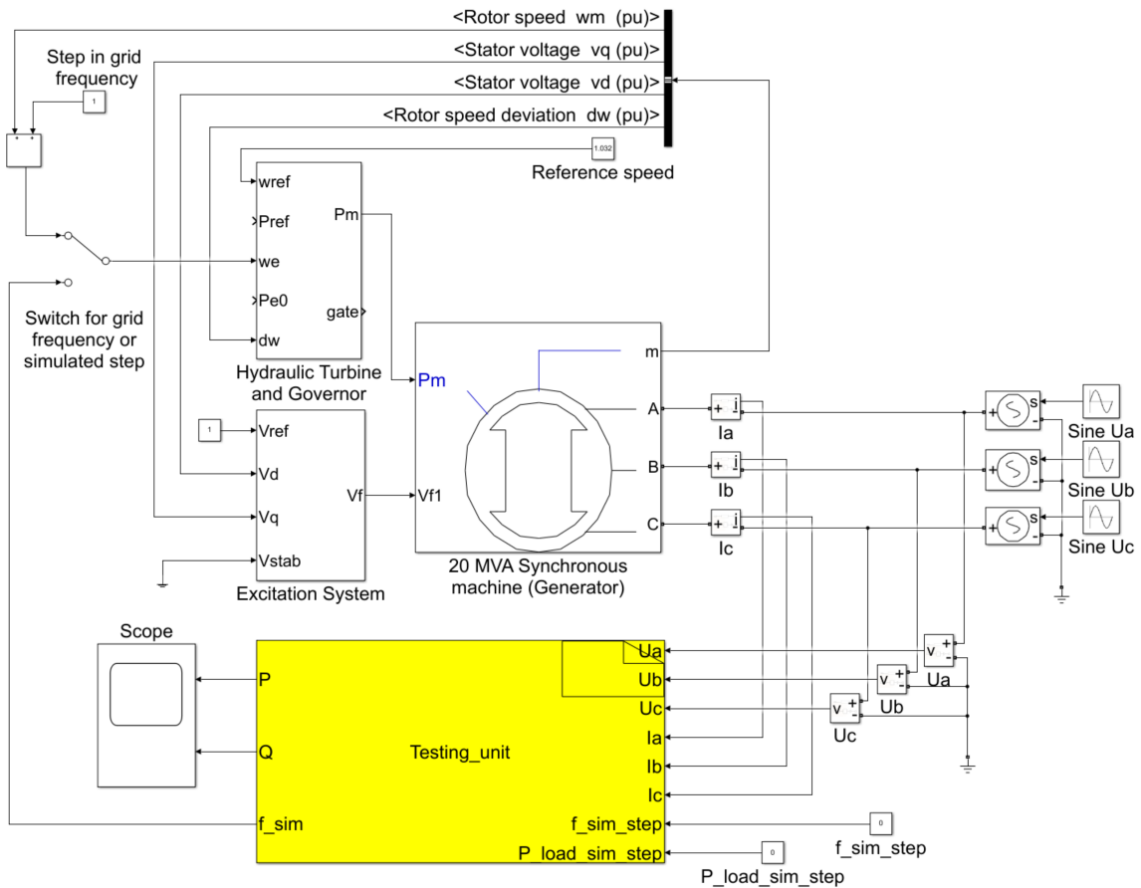


Figure 5.4: Simulink model of the power-generating module and the testing module.

The code in the testing unit is implemented in Simulink via a s-function block. The block is initializing, updating and terminating variables defined in the c-code using the c-code methods while at the same time updating the variables in Simulink. The voltages and currents from the simulated power-generating module is then sent to the s-function block and P and Q are obtained at the output.

To provide the governor with the simulated frequency signal from the testing unit block instead the normal rotor speed is switched to f_{sim} . Depending on if the unit is set to open or closed loop operation the steps set by the user are done with changing the variables $f_{sim,step}$ or $P_{Load,sim,step}$.

The parameters used for frequency control described in Section 2.5 are implemented in the block Hydraulic Turbine and Governor are selected to the suggested standard parameters for a power generating module in [19] shown in Table 5.4 and 5.5. To show different tunings of the power-generating module the value of K_i is changed for different simulations.

Table 5.4: Selected parameters in the generator of the Simulink model.

Generator parameter	Nominal power P_n	Rated voltage V_n	Stator resistance R_s	Inertia constant H	Pole pairs p
Value	20 MW	10 kV	0.002 pu.	3 s	2

Table 5.5: Selected parameters in the governor of the Simulink model.

Governor parameter	Permanent Droop R_G	Proportional K_p	Integrator Open loop K_i	Integrator Closed loop K_i	Droop reference
Value	4%	2.5	0.7	0.07	Gate position

The steady state active power of the power-generating module in the Simulink model is set to be 0.8 pu.

When testing for FCR, the frequency tested is in the range of 49.5-50.5 Hz i.e. 1 ± 0.01 pu. To increase resolution of the input signal to the governor in the model, the limited voltage output of ± 10 V of the testing unit is therefore be scaled to fit the testing frequency deviation from 50 Hz as seen in Table 5.6. This means that the ratio of the output voltage and frequency change is set to 0.05 Hz/V.

The voltage and frequency range for the Simulink simulation is shown in Table 5.6.

Table 5.6: Testing unit DAC output voltage and corresponding frequency value for simulated governor input.

	Min	Steady state	Max
Testing unit DAC	-10 V	0 V	10 V
Simulated frequency	49.5 Hz	50 Hz	50.5 Hz

5.3.2 Simulation environment and software to hardware interface

To get a real-time-interface and measurable analog voltage signals ControlDesk and MicroLabBox from dSPACE are used. MicroLabBox is an electronic control unit (ECU) and ControlDesk its instrumentation software.

The MicroLabBox has 16 analog output cannels and 8 analog input channels with a voltage range of ± 10 V all provided with a BNC-connector. The 10kV voltage and ~ 1.6 kA current that the power-generating module is being run at in steady state needs to be scaled down to fit the hardware. The Simulink model also needs to be modified with certain dSPACE DAC and analog-to-digital converter (ADC) blocks, for communication the hardware. It is then compiled into ControlDesk where all the variables are monitored and controlled.

The testing unit samples data at a rate of 2 kHz and the MicroLabBox is set to a sampling rate of 20 kHz. The reason is to have better accuracy and higher resolution of the real time simulations processed in ControlDesk. For the comparison of the results every 10:th sample of the ControlDesk-file is compared to the one from the testing unit.

5.3.3 Amplifier equipment

The TC.ACS by REGATRON is a multi-level inverter acting as a full 4 quadrant 3-phase alternating current (AC) power source. Running it in amplifier mode and connecting the outputs from the MicroLabBox to TC.ACS will amplify the voltage to the desired value. The technical specification of the TC.ACS is presented in Table 5.7.

Table 5.7: TC.ACS technical specification.

Type	Rating	Accuracy
Voltage at 50/60 Hz	-	0.05% FS
Voltage output	0-300 $V_{rms,L-N}$	<1.5 V
Phase angle	-	1°
Frequency	0-1000 Hz	2 mHz

6

Results

This chapter contains the results of simulations and measurements, recorded simultaneous for every test case, in graphs for different operation modes and control signals.

6.1 Precision tests

This section contains results from tests described in Section 5.1, performed to verify the precision of the testing unit's measurements.

Figure 6.2 shows a raw measurement of the phase voltage U_b sampled with 2 kHz. The provided voltage of the OMICRON CMC 356 is 10 $V_{V-L,RMS}$ with a frequency of 50.1 Hz. The same pattern of a fluctuating top-value is seen in all phase voltage and current measurements.

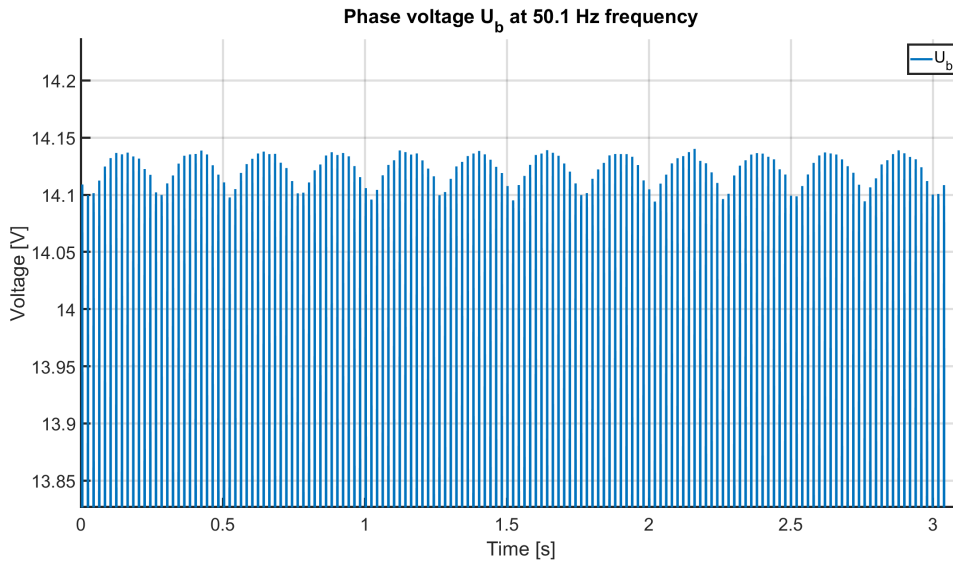


Figure 6.1: Phase voltage U_b at 50.1 Hz, with 2 kHz sampling frequency.

Figure 6.2 shows sampled 2 kHz value of the testing unit being provided with 10 $V_{L-N,RMS}$ and 1 A with a frequency of 50 Hz continuously. The mean measured frequency is 50.0005 Hz with peak-to-peak fluctuations of 0.0003 Hz. The mean active power is 29.9979 W with fluctuations of 0.04 W.

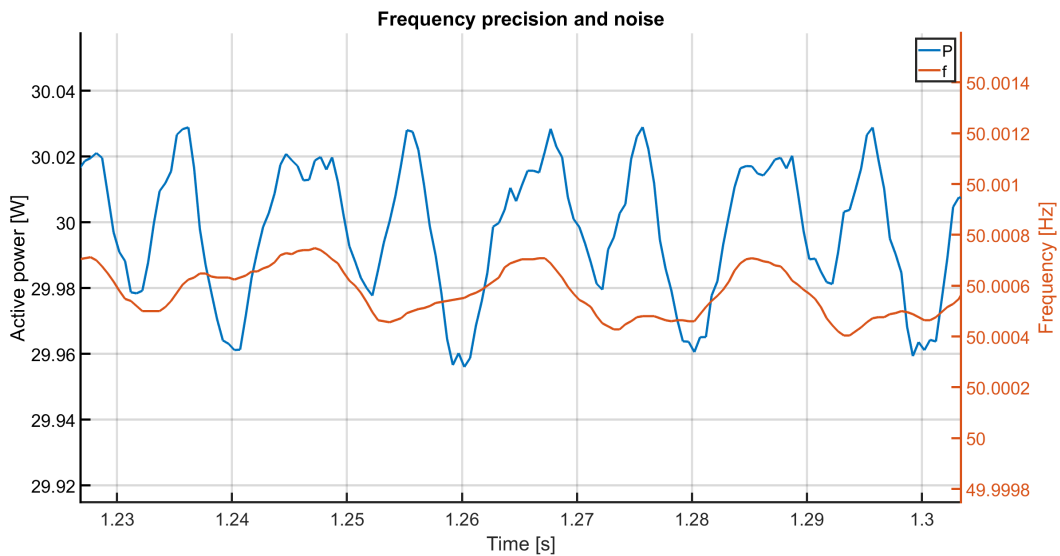


Figure 6.2: Active power and frequency sampled at 2 kHz.

Figure 6.3 presents a sequence where the voltage and frequency are stepped. The voltage steps are done with changing the voltage from $10 V_{V-L,RMS}$ to $20 V_{V-L,RMS}$, one when the frequency is 50 Hz and one where the frequency is 50.5 Hz. The response in active power measurement is instant and the rise time of the frequency change is 0.148 seconds.

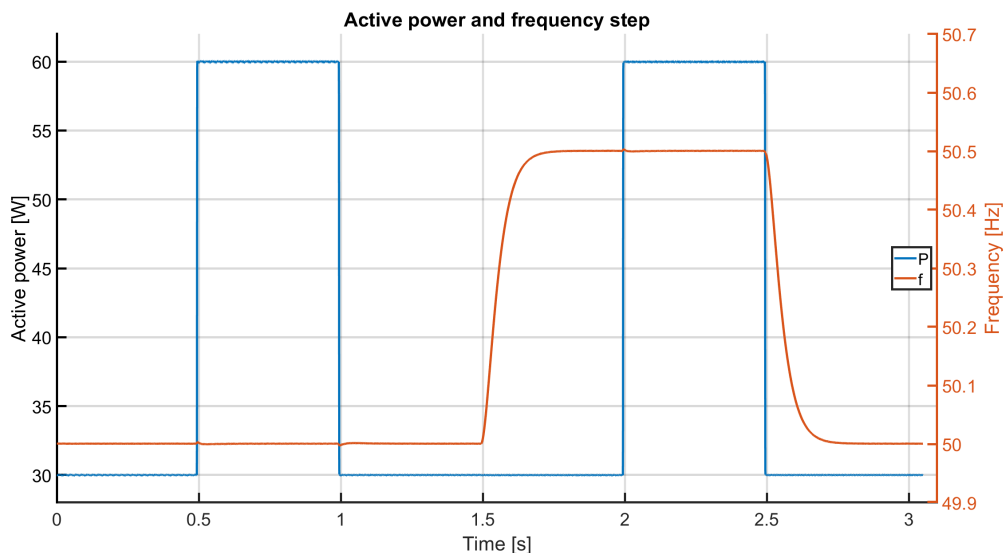


Figure 6.3: Step of active power and frequency with an output sample rate of 2 kHz.

For Figure 6.4 the same procedure for the sequence is followed. The difference is the down sampling of the output values and hence longer test described in Section 4.1.1. The frequency step appears instant due to change of sampling rate.

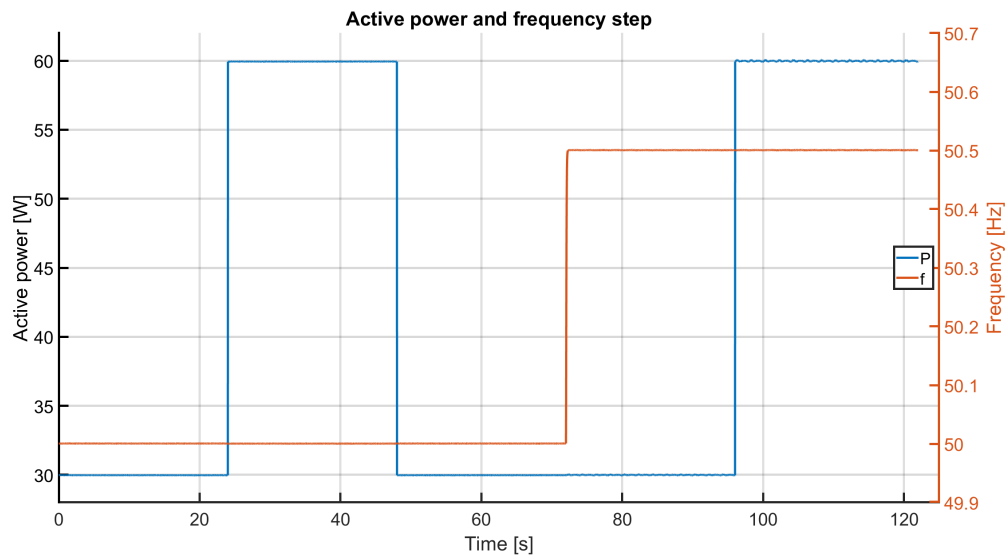


Figure 6.4: Step of active power and frequency with an output sample rate of 50 Hz.

Looking closely at the active power when the frequency is 50.5 Hz shows small fluctuations but not when the frequency is at 50 Hz.

As soon as the frequency deviates from 50 Hz the magnitude of the voltage and current measurements fluctuates for the long tests. The fluctuation appears to be linear with the deviation from the nominal frequency, Δf , and have the same pattern as the noise shown in Figure 6.2. Figure 6.5 shows a close up of the fluctuation, for a Δf of 0.005 Hz and 0.1 Hz.

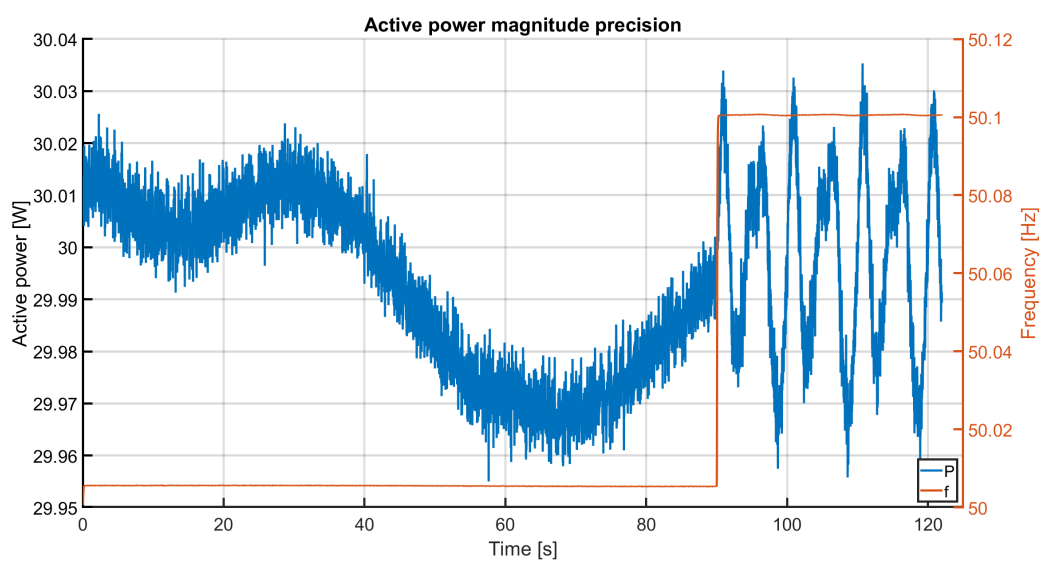


Figure 6.5: Active power at frequencies of 50.005 Hz and 50.1 Hz consecutively, sampled at 2 kHz and then being down-sampled to 50 Hz.

6.2 Grid tests

For the grid tests the procedure described in Section 5.2 is followed. Figure 6.6 shows the active power consumed by the resistive loads and the frequency deviations of the frequency in the grid. The active power consumed is fluctuating due to voltage fluctuations.

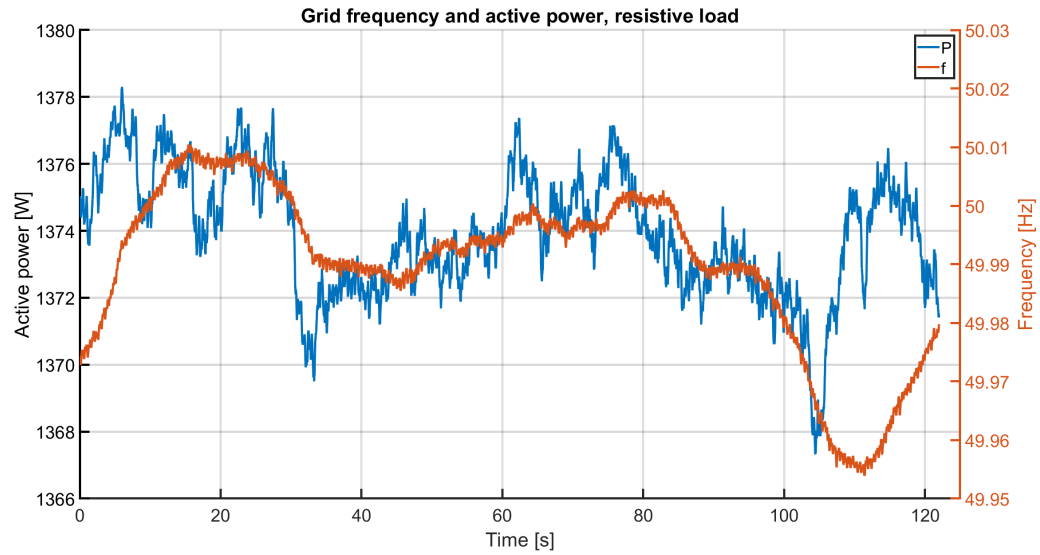


Figure 6.6: Active power and frequency of resistive load connected to grid, sampled with 2 kHz.

6.3 Application tests

The following figures shows the results from the setup described in Section 5.3. Figure 6.7 shows a deviation in the measured active power that is seen for all plots in Section 6.3. The reason to it is discussed in Section 7.1 but for the results the graphs are modified to be on top of each from the start of the measurement shown in Figure 6.8. The offset is compensated by calculating the average difference between the measured and simulated values in the 2.5-3.5 sec range and applying it to the measured values. This gives the ability to study if the measurements follow the simulated results.

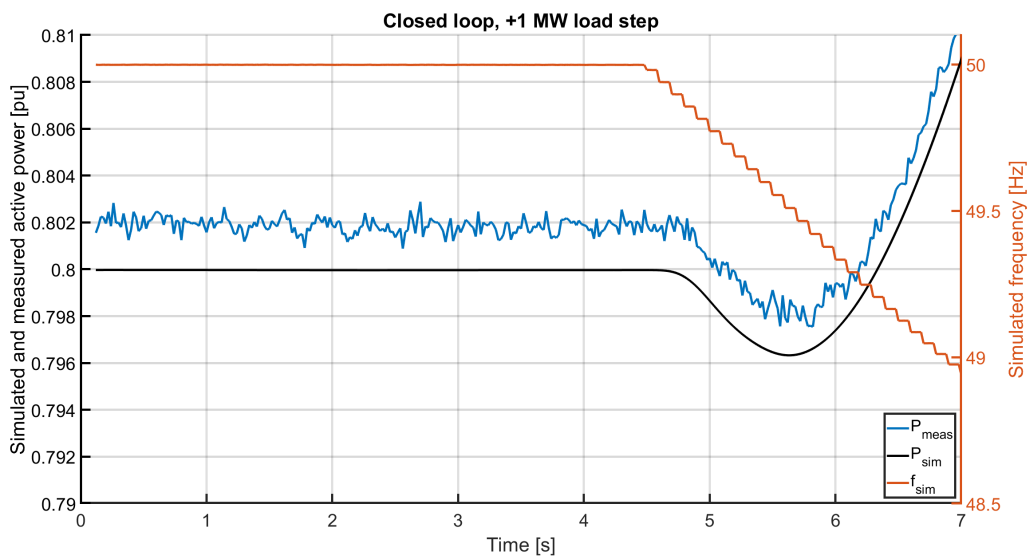


Figure 6.7: Steady state active power with offset between simulated and measured values.

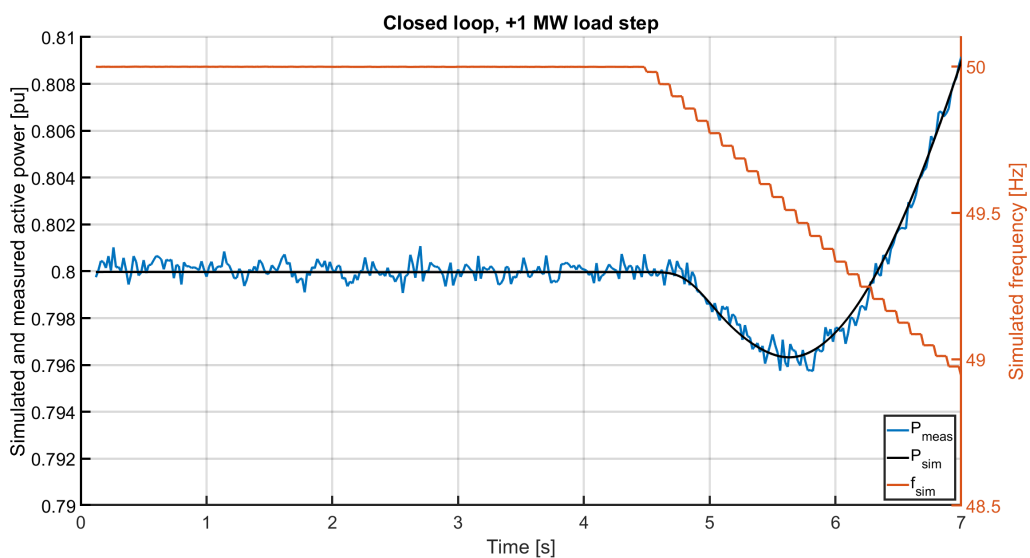


Figure 6.8: Steady state active power with compensated offset.

6.3.1 Open loop operation

This section shows the application tests for open loop operation of the testing module described in Section 3.1. For all figures in this section, except for Figure 6.20, K_i is set to 0.7.

Figure 6.9 shows a step of +0.1 Hz in the simulated frequency signal. The measured active power deviates from the simulated one as time proceeds. The simulated curve is going towards the steady state value of 0.75 pu. and the measured exceeds the expected value after 110 seconds.

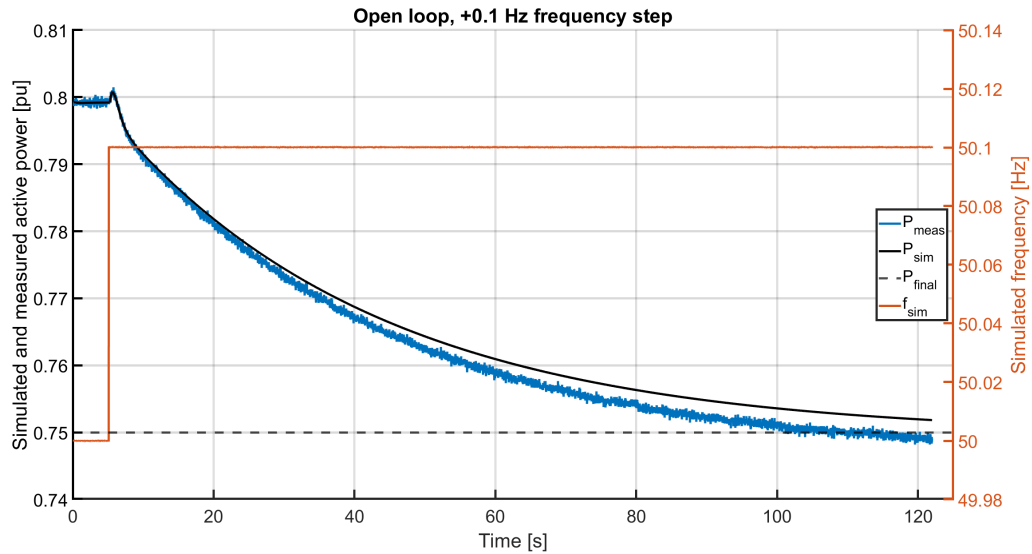


Figure 6.9: +0.1 Hz frequency step with open loop operation of the testing unit.

In Figure 6.10 the applied frequency step is +0.2 Hz which results in a similar response as in the last figure. The regulation reaches the same offset between the expected steady state value and the simulated steady state value in pu. in the same amount of time. The measured active power is deviating as time proceeds just as in Figure 6.9.

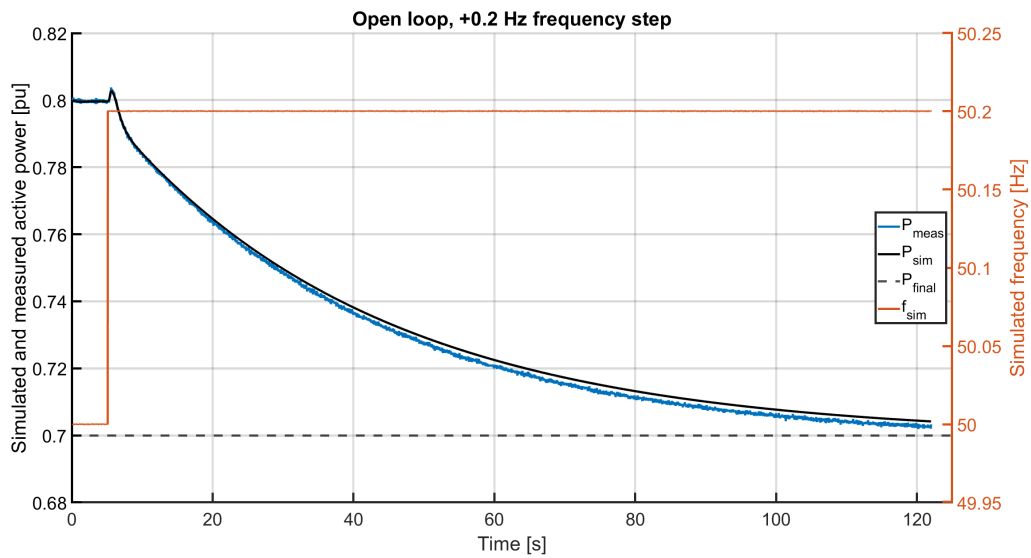


Figure 6.10: +0.2 Hz frequency step with open loop operation of the testing unit.

In Figure 6.11 the frequency step is +0.5 Hz and the expected steady state value of the active power is 0.55 pu.

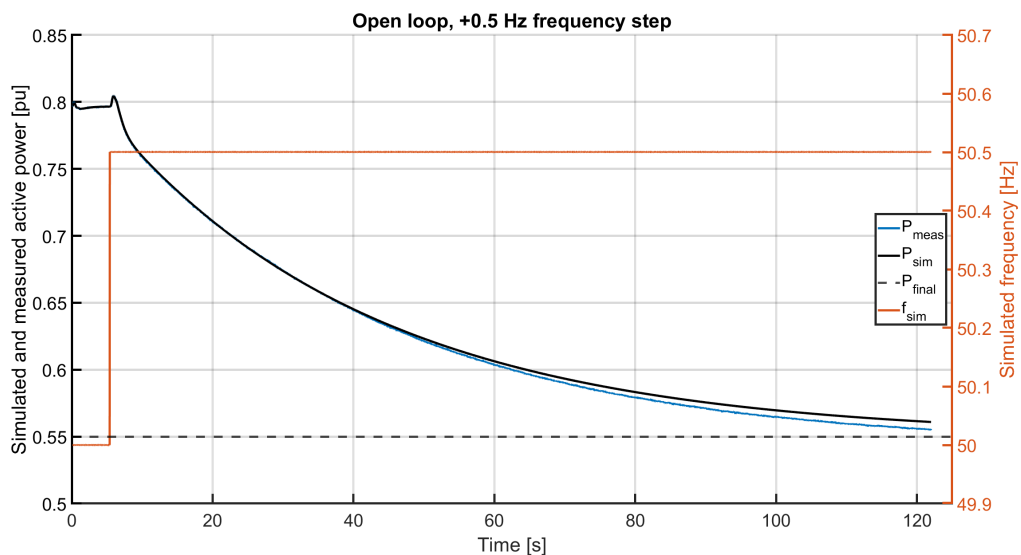


Figure 6.11: +0.5 Hz frequency step with open loop operation of the testing unit.

In Figure 6.12 the system is instead experiencing a negative frequency step of -0.1 Hz which shows a similar active power response as in Figure 6.9, but in the opposite direction. The deviation of measured active power is positive compared to negative earlier.

6. Results

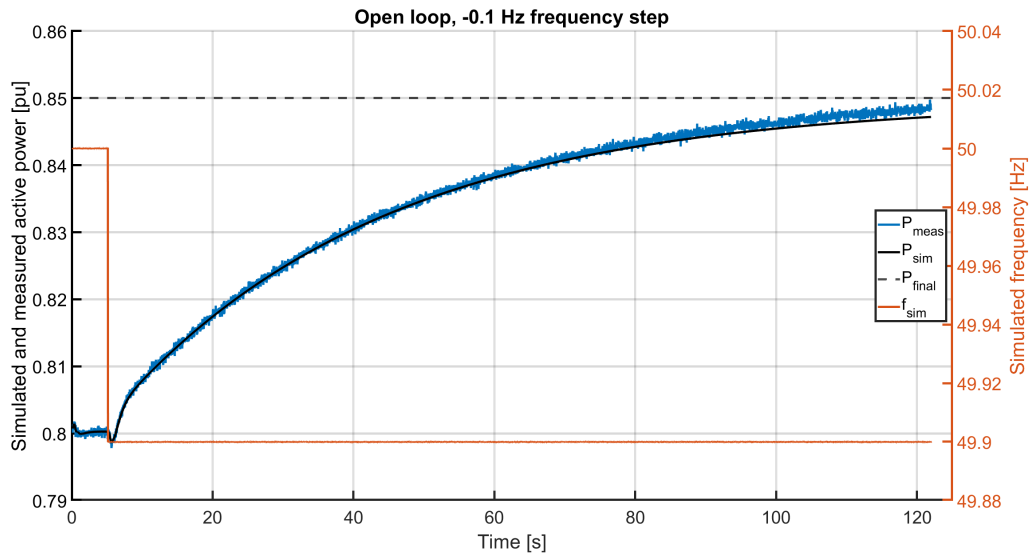


Figure 6.12: -0.1 Hz frequency step with open loop operation of the testing unit.

Figure 6.13 shows a frequency step of -0.5 Hz. The expected steady state power is 1.05 which exceeds the rated output of 1 pu. of the power-generating module. The power-generating module outputs the rated power for the rest of the test. The measured active power is larger than the simulated on.

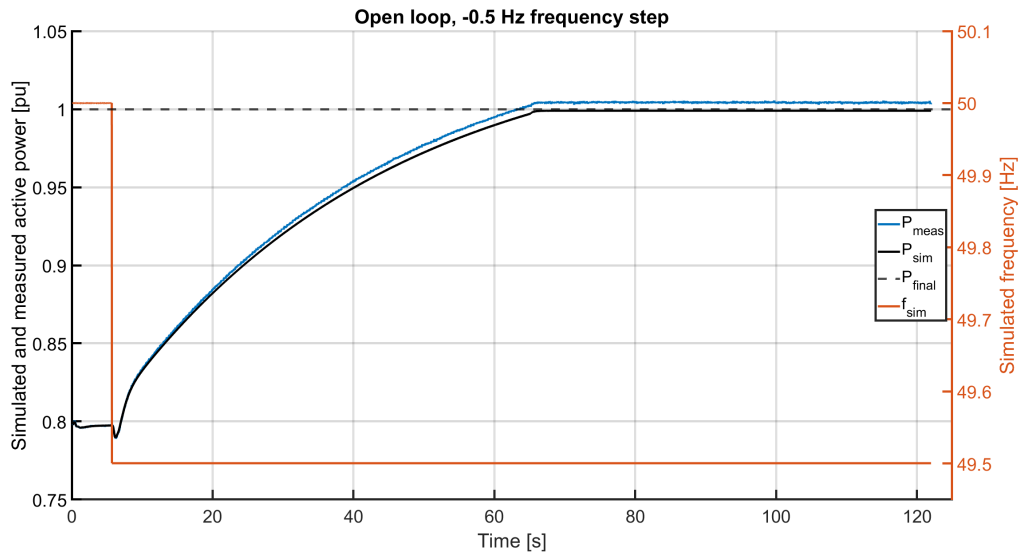


Figure 6.13: -0.5 Hz frequency step with open loop operation of the testing unit.

The measured and simulated active power when reaching rated capacity can be seen closer in Figure 6.14 below. The measured active power, P_{meas} , for the last 40 seconds is almost constant 1.0042 pu, while the simulated active power, P_{sim} , is almost constant 0.9990 pu. The difference here compared to all figures above is that the derivative of the deviation for the simulated and measured active power is zero when the derivative of the active power is zero.

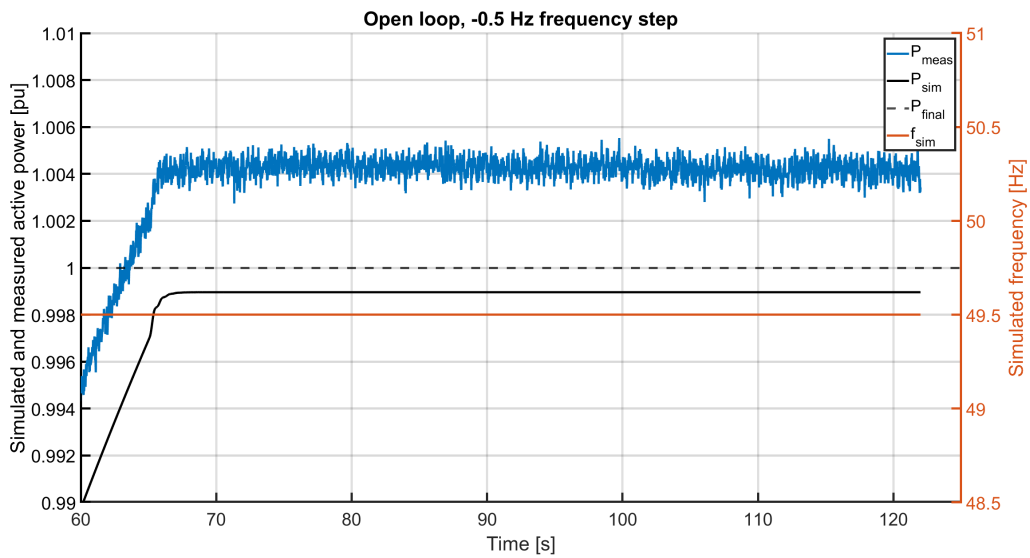


Figure 6.14: -0.5 Hz frequency step with open loop operation of the testing unit after reaching maximum capacity.

In Figure 6.15 a step of +0.1 Hz is applied, followed by a step of -0.2 Hz. For the negative step the measured active power is lower than the simulated and for the positive step it is higher.

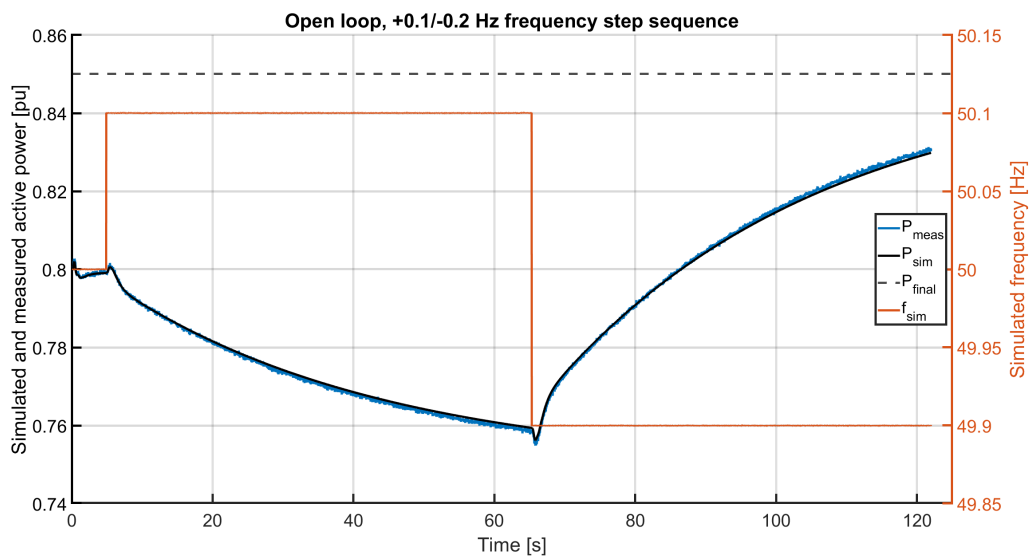


Figure 6.15: +0.1 and -0.2 Hz frequency step sequence with open loop operation of the testing unit.

In Figure 6.15 a step of +0.2 Hz is applied, followed by a step of -0.3 Hz. The active power deviation between simulation and measured follow the same pattern as above.

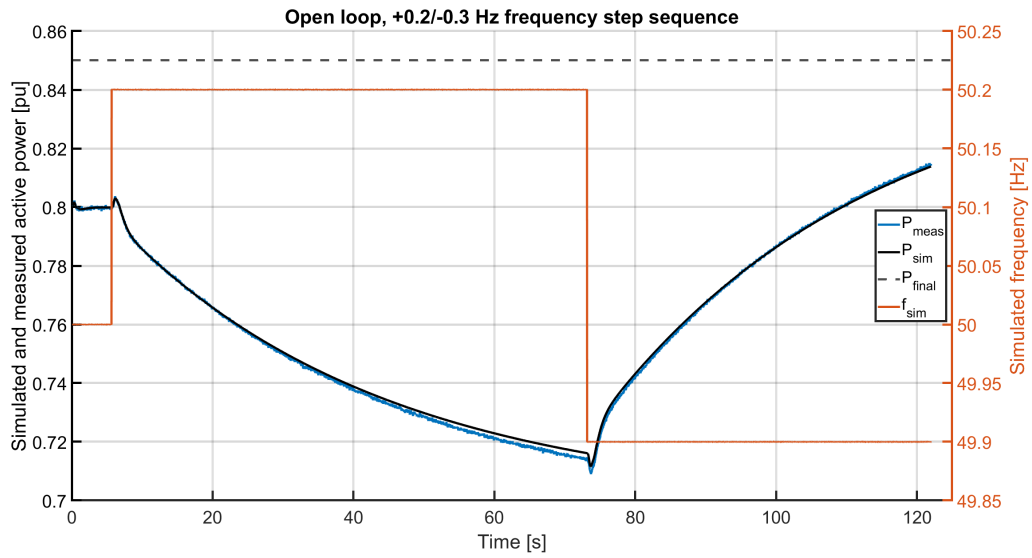


Figure 6.16: +0.2 and -0.3 Hz frequency step sequence with open loop operation of the testing unit.

In Figure 6.17 an imposed sinusoidal frequency is applied as input for the turbine governor. The sinusoidal change has an amplitude of ± 0.1 Hz and a period time of 60 sec. The frequency signal oscillates stable around 50 Hz but the active power response average value increases due to longer time delays for opening of the water gates than for closing. The response is still sinusoidal though.

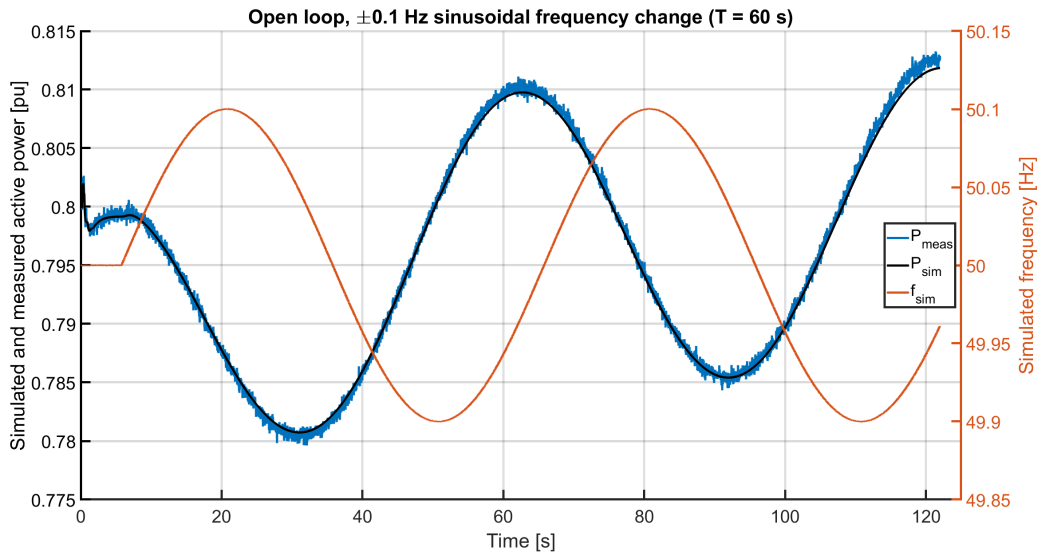


Figure 6.17: 60 sec period time imposed sinusoidal frequency change with amplitude deviation of ± 0.1 Hz, with open loop operation of the testing unit.

Figure 6.18 shows the same sinusoidal frequency input but with a period time of 30 seconds.

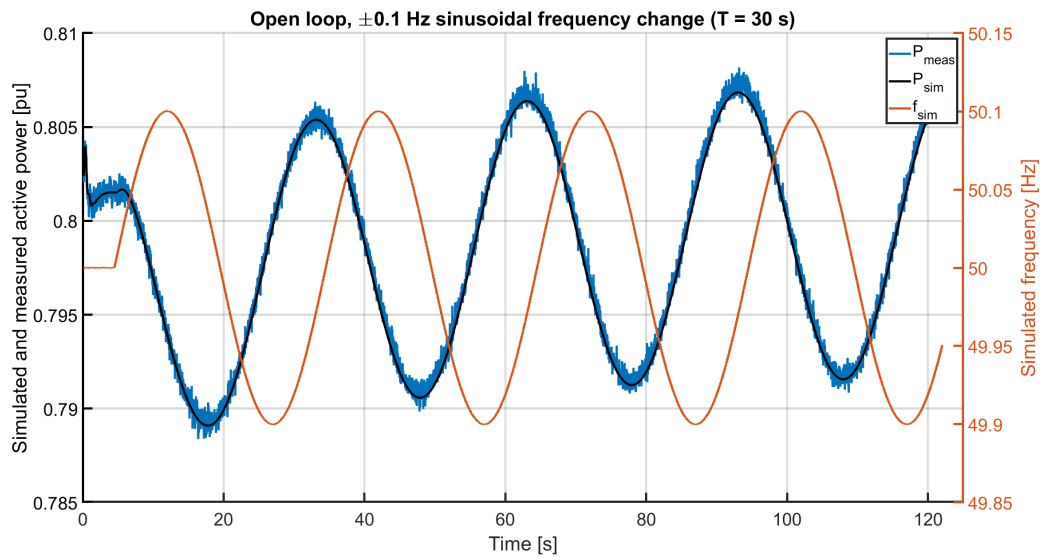


Figure 6.18: 30 sec period time imposed sinusoidal frequency change with amplitude deviation of ± 0.1 Hz, with open loop operation of the testing unit.

In Figure 6.19 the sinusoidal frequency change has an amplitude of ± 0.2 Hz and a period time of 10 sec.

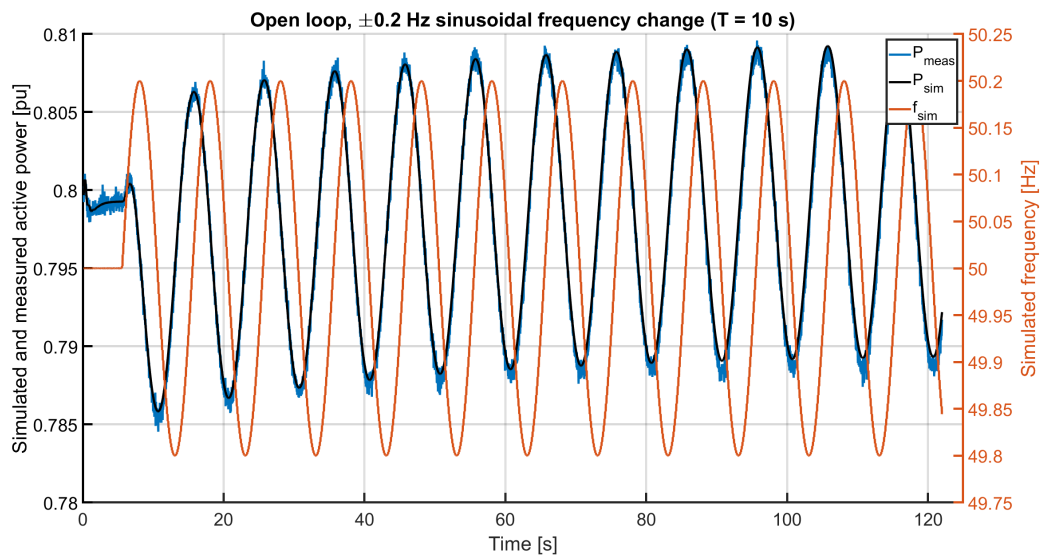


Figure 6.19: 10 sec period time imposed sinusoidal frequency change with amplitude deviation of ± 0.2 Hz, with open loop operation of the testing unit.

For Figure 6.20 the value of K_i in the governor is changed to 0.07 and a step in the frequency of $+0.1$ Hz is applied. The governor now reacts slower compared to the same step applied in Figure 6.10. The difference compared to the other figures in the section is that the measured power is higher than the simulated one even though the power has a negative derivative.

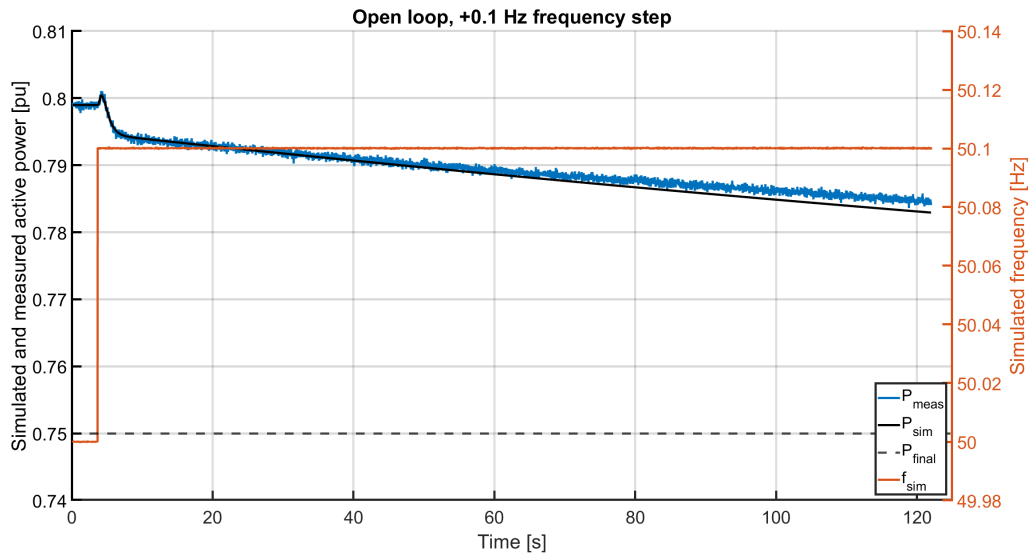


Figure 6.20: +0.1 Hz frequency step with open loop operation of the testing unit with governor parameter K_i set to 0.07.

6.3.2 Closed loop operation

This section shows the application tests for closed loop operation of the testing module described in Section 3.2. The value of K_i is kept at 0.07.

Figure 6.21 shows the response for a load step of -1 MW. Notice the simulated frequency calculation in the orange line. The expected steady state value is 0.75 pu. and the power-generating module reaches it after 22 seconds.

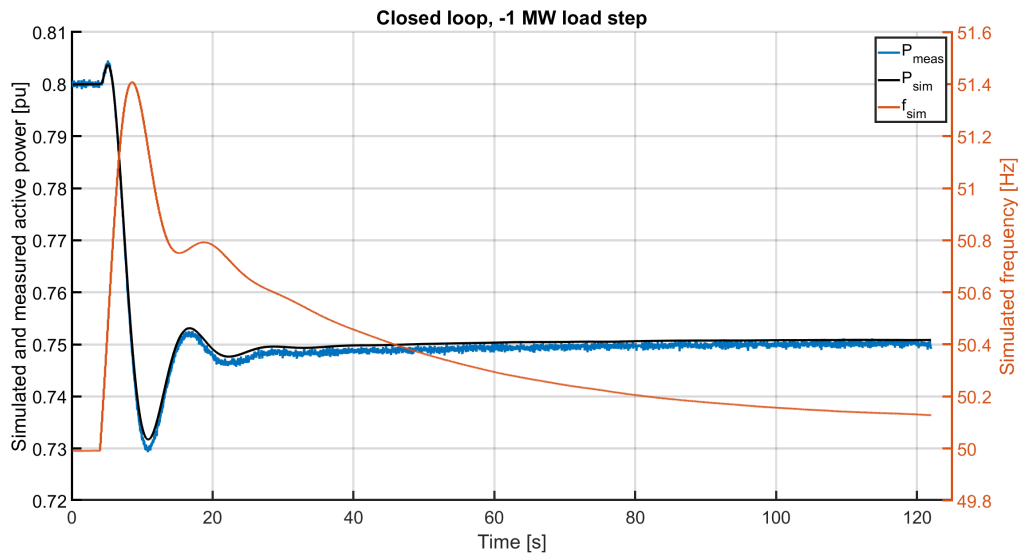


Figure 6.21: -1 MW load step with closed loop operation of the testing unit.

Figure 6.22 shows a load step of +1 MW and the result is similar to the previous one. The measured power is at the start of the steady state value higher than the simulated

ones but as time continues it decreases to a value lower than the simulated. Figure 6.23 shows a close up of the crossing.

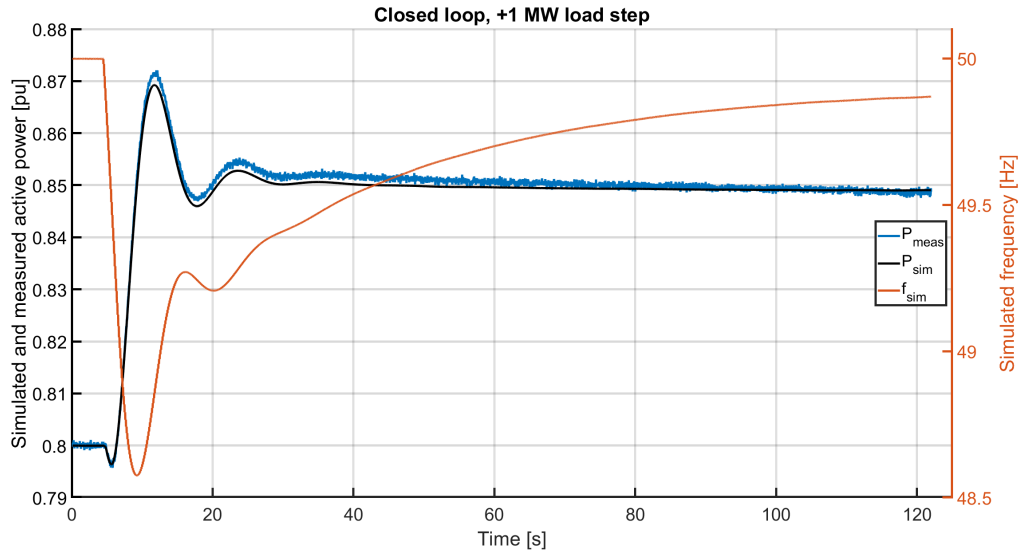


Figure 6.22: +1 MW load step with closed loop operation of the testing unit.

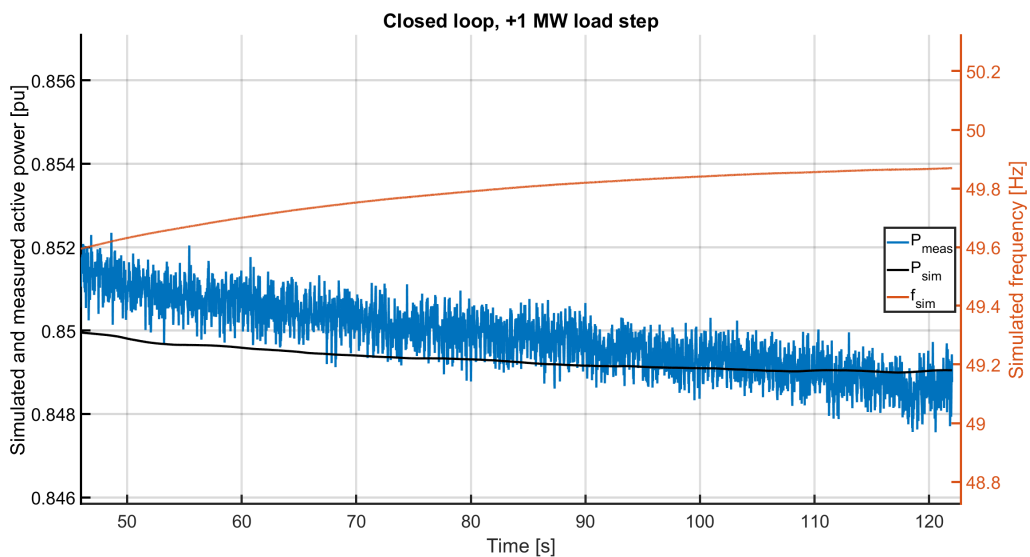


Figure 6.23: +1 MW load step with closed loop operation of the testing unit. Simulated and measured active power crossing.

The value of K_i is changed to 0.7 and a step of -1 MW is applied seen in Figure 6.24. The output response is with this parameterisation is more volatile than in Figure 6.21 and the steady state is never reached during the simulation.

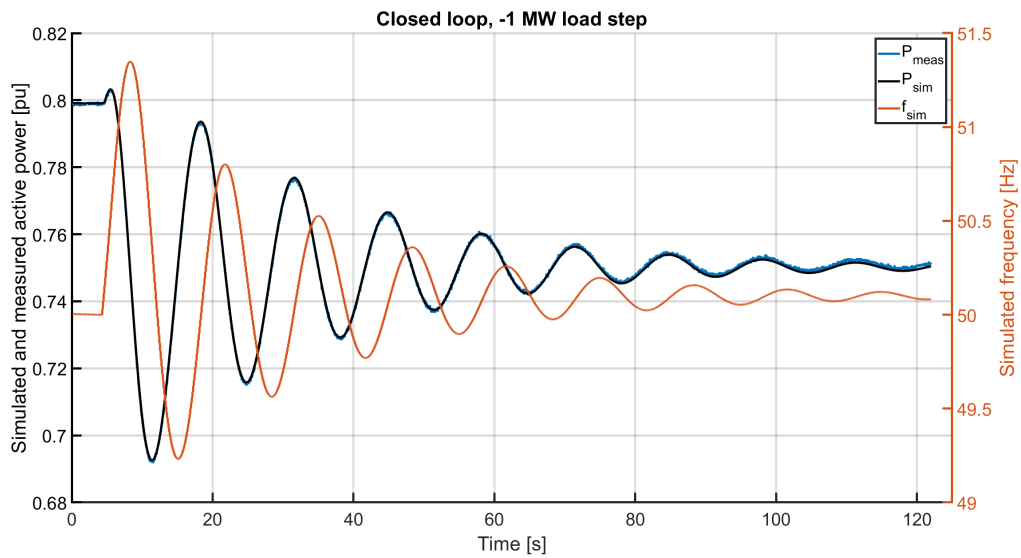


Figure 6.24: -1 MW load step with closed loop operation of the testing unit with governor parameter K_i set to 0.7.

Figure 6.25 shows a load step of +1 MW with the same K_i . The difference in response from Figure 6.24 is the delay of opening and closing the water valves.

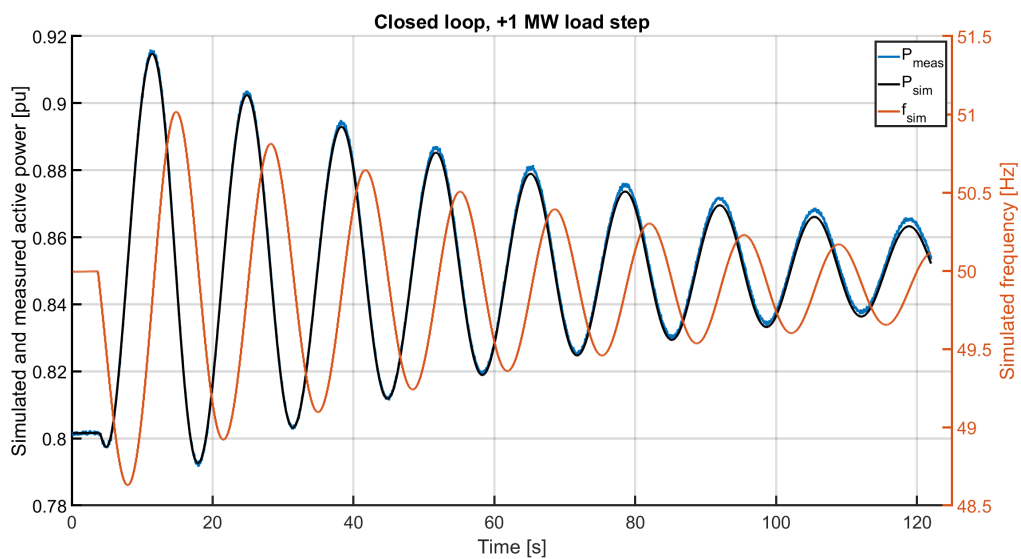


Figure 6.25: +1 MW load step with closed loop operation of the testing unit with governor parameter K_i set to 0.7

7

Discussion

The discussion chapter includes the thoughts of why the results are the way they are. The deviations between expected values and measured values are discussed below.

7.1 Precision of measurements

As seen in Figure 6.5 the magnitude of the active power fluctuates when the frequency deviates from the nominal 50 Hz. It fluctuates with the same pattern as the noise in the measured active power seen in Figure 6.3 and can be seen in all values transformed into the dq-frame. The noise is for all the tests done, occurring with the same frequency as the phase voltages and currents. If they have a frequency of 50.1 Hz the noise is 50.1 Hz and if the frequency is 50.5 Hz the noise is 50.5 Hz. When the output file is down-sampled to 50 Hz, the sample will hit the noise on different places along the curve. It will then appear as a floatation with a period time linear to the deviation from the nominal frequency, Δf . To get a more stable measurement of the active power the noise seen in the Figure 6.3 can be filtered out. Applying the filter described in Section 4.4.5 with a $\alpha = 0.06$ to the active power measurements, sampled at 2 kHz, is sufficient to get rid of the noise. In Figure 7.1 below, the filter has been implemented and been placed on top of Figure 6.5 before down-sampling to 50 Hz resulting in the black curve, $P_{filtered}$.

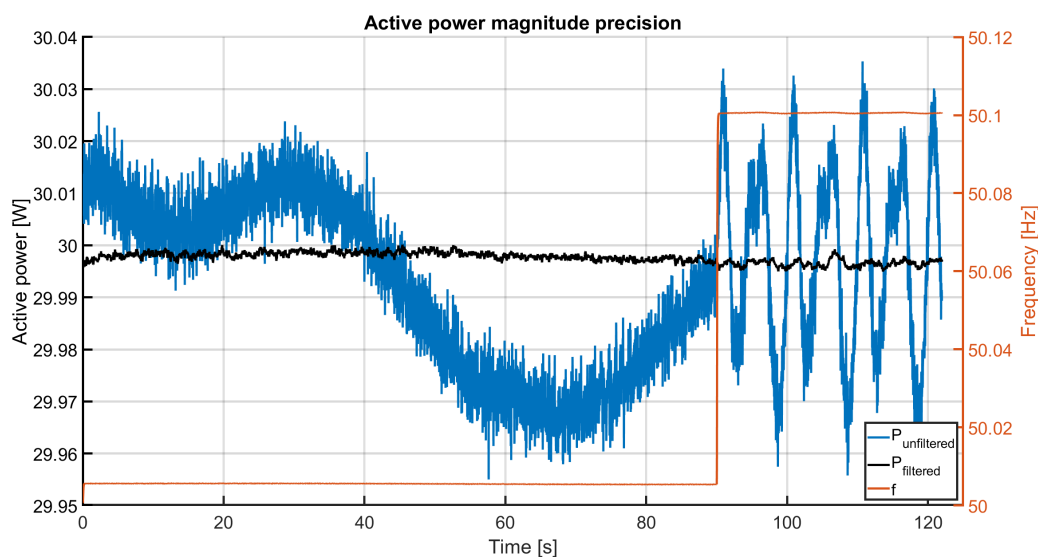


Figure 7.1: Active power at frequencies of 50.005 Hz and 50.1 Hz consecutively sampled at 2 kHz, unfiltered and filtered, being down-sampled to 50 Hz.

Doing this for all measurements would stabilize the active power measurements.

7.2 Deviation between measured and simulated values in the application testing

There are two discussable matters of the application test results.

- Why does the measured active power deviate from the simulated one in Figure 6.8?
- Why does the measured value deviate more from the simulated one when the power deviates more from the initial 0.8 pu.?

The offset between the initial measured and simulated active power can origin from two sources. The expected output voltages of the TC.ACS and MicroLabBox when the power-generating unit is in steady state is $80 V_{L-N,RMS}$ and $5.65 V_{L-N,RMS}$ respectively. In simulation values are correct but if the terminal voltage of the TC.ACS is measured it shows a lower voltage than expected. The three phase resistors used in the circuit are not accurately 50Ω . The value of them also change due to temperature. These two in combination creates an offset that is difficult to calibrate when the measured value fluctuates as in Figure 6.5.

The answer to the second question is more unclear. Two patterns are to be seen from the results. The first is that the offset in measured active power deviates more from the simulated values the further away from the original steady state it gets. The inaccuracy of the measurement is not linear with the change of active power steady state values in all results but the difference is small. This is also motivated with the result in Figure 6.14 where the deviation of measured and simulated values stays at a constant deviation from each other when the change of active power is zero.

The second pattern seen is a Figure 6.20, 6.21, 6.23 and especially in Figure 6.23. When the power-generating module is close to the new steady state value for a longer duration the active power starts to float. When trying to find the origin the value of φ also has been noticed floating. A φ deviating from zero means that there is reactive power flowing even though the circuit is fully resistive. An explanation can be that the different voltage sources deviate a bit in the clock oscillators they are run by. It will appear in the measurement as a "phase-shift" between the voltage and current that is going back and forth from each other with a long period time. The limited storage capacity prevents it to be studied further due to assumed longer floatation than 122 seconds.

7.3 Simulated power-generating module or real power-generating module

The chosen method to simulate voltages and currents and providing them with power electronic equipment differs from measuring on a real power-generating module. The pros of it is that it's a safe and flexible way where equipment doesn't risk to be damaged and parameters easily can be changed. The cons are that the deviations and inaccuracies of

measurements are explained by other reasons.

The Simulink model has been a perfect tool to study a power-generating module's dependency on different parameter values. The usage of testing the code under ideal conditions has been a perfect way to get a hint if it's going to work or not. It's also been easy to compile into ControlDesk.

The case of using different sources for provision of voltage and current may cause different magnitude deviations or phase positions from each other due to delays and noise of the equipment. Measuring with voltage and current transformers on a real power-generating module has the benefit that the signals come from the same analog source.

7.4 Importance of parametrisation of the governor

For frequency regulation, the results shows the importance of having a tuned parametrisation of the governor. For open loop operation of the testing unit and the K_i value set to 0.7 the power-generating module would be approved for FCR-N but not for FCR-D according to the technical requirements in Section 2.3. For the closed loop operation the technical requirements are unknown but it's clearly seen that a value of K_i set to 0.07 is more stable and has a faster regulation compared to the ones with K_i set to 0.7.

7.5 Future studies

To improve the testing unit it's suggested to apply the filter described in 7.1 and tune it to it's application to ensure a better accuracy.

To improve the application tests setup it's suggested to find the reasons to the inaccuracies of the measured active power from the TC.ACS or the MicroLabBox.

The next step would be to test the unit on a real power-generating unit and study the differences.

8

Conclusion

In this chapter the results are compared to the technical requirements and to the aim.

The testing unit is able to meet the technical requirements for testing of FCR provision in the Nordic synchronous area. The requirements states that the instantaneous power measurements must have a minimum accuracy of 0.5 % of the rated power of the providing entity, which the results from precision testing of the testing unit holds true. The frequency measurement requirements of 1 mHz resolution and 10 mHz accuracy is also met by the testing unit, with a resolution of < 0.2 mHz and accuracy of < 1 mHz, from the precision tests.

The aim of the report, to develop a testing unit able to test the frequency controlling performance of a power-generating module, is accomplished.

Bibliography

- [1] N. Ung, “The effects of backlash on the frequency stability in a hydro based power system,” [Online]. Available: <http://www.svk.se/siteassets/jobbar/dokument/the-effects-backlash-on-frequency-stability-in-hydro-based-power-system.pdf>.
- [2] H. Engel, R. Hensley, S. Knupfer, and S. Sahdev, “The Potential Impact of Electric Vehicles on Global Energy Systems,” *McKinsey Center for Future Mobility*, no. Exhibit 1, p. 8, 2018. [Online]. Available: <https://www.mckinsey.com/industries/automotive-and-assembly/our-insights/the-potential-impact-of-electric-vehicles-on-global-energy-systems>.
- [3] ENTSO-E, “Nordic Report: Future System Inertia,” *Nordic Report*, pp. 1–58, 2017. [Online]. Available: https://www.entsoe.eu/Documents/Publications/SOC/Nordic/Nordic_report_Future_System_Inertia.pdf.
- [4] E. Agneholm, N. Krantz, M. Emanuelsson, H. Hermansson, S. Ab, S. Kraftnät, and V. A. Elproduktion, “Solvsim Power Station – a New Safe Way of Testing the Frequency Control and Island Operation Capability of Power Stations,” 2002. [Online]. Available: http://pscc.ee.ethz.ch/uploads/tx_ethpublications/s06p06.pdf.
- [5] European Union, “Commission Regulation (Eu) 2016/631,” *Official Journal of the European Union*, no. 14 April 2016, p. 68, 2016.
- [6] “Energimarknadsinspektionens författningssamling Energimarknadsinspektionens föreskrifter nätanslutning av generatorer ;,” 2018. [Online]. Available: https://www.ei.se/Documents/Publikationer/foreskrifter/EI/EIFS_2018_2.pdf.
- [7] Fingrid, “Frequency Quality Analysis 2019 FINGRID,” 2019. [Online]. Available: <https://www.fingrid.fi/en/grid/power-transmission/maintenance-of-power-balance/>.
- [8] M. Kuivaniemi, *Frequency - historical data [CSV-file from Fingrid Oyj]*. [Online]. Available: <https://data.fingrid.fi/en/dataset/frequency-historical-data>.
- [9] Svenska Kraftnät, “Årsredovisning 2019,” 2019. [Online]. Available: <https://www.svk.se/press-och-nyheter/nyheter/allman-nyheter/2020/arsredovisning-2019/>.
- [10] —, “Ödrift - För att säkerställa elförsörjning i krissituationer,” [Online]. Available: <https://www.svk.se/sakerhet-och-hallbarhet/elberedskap/>.
- [11] IEEE board, “IEEE Policies 2014,” no. February, 2014. [Online]. Available: <https://www.ieee.org/about/corporate/governance/p7-8.html>.

- [12] P. Chen, *PSAC SS5b FrequencyRestorationProcess [PowerPoint slides]*, 2020.
- [13] Svenska Kraftnät, “Villkor för FCR,” vol. 1, no. 16, pp. 1–16, [Online]. Available: <https://www.svk.se/aktorsportalen/elmarknad/balansansvar/balansansvarsavtal/>.
- [14] P. W. Group, “Supporting Document on Technical Requirements for Frequency Containment Reserve Provision in the Nordic Synchronous Area Draft 2017 Prequalification Working Group , FCP project THE REQUIREMENTS ARE SO FAR DRAFT REQUIREMENTS,” no. June, 2017.
- [15] “Turbine Governor Test Equipment,” no. July, pp. 1–30, 2019.
- [16] F. Fjærterminal, “Feldetektor och Fjærterminal,” 2005. [Online]. Available: https://www.protrol.se/uploaded_files/IPC4020_datablad_2005_se1.pdf?v20200515104610.
- [17] L. Harnefors, “Control of Variable-Speed Drives,” *Applied signal processing and control department of electronics, Mälardalen university*, 2002.
- [18] M. Bongiorno, J. Svensson, and A. Sannino, “Effect of sampling frequency and harmonics on delay-based phase-sequence estimation method,” *IEEE Transactions on Power Delivery*, vol. 23, no. 3, pp. 1664–1672, 2008, ISSN: 08858977. DOI: 10.1109/TPWRD.2008.915802.
- [19] P. Kundur, *Power System Stability And Control*, 1994.